

July 2017

BURROWING AND WALKING MECHANISMS OF NORTH AMERICAN MOLES

YI-FEN LIN
University of Massachusetts Amherst

Follow this and additional works at: https://scholarworks.umass.edu/dissertations_2



Part of the [Biomechanics Commons](#), [Evolution Commons](#), [Integrative Biology Commons](#), [Other Ecology and Evolutionary Biology Commons](#), and the [Zoology Commons](#)

Recommended Citation

LIN, YI-FEN, "BURROWING AND WALKING MECHANISMS OF NORTH AMERICAN MOLES" (2017). *Doctoral Dissertations*. 921.
https://scholarworks.umass.edu/dissertations_2/921

This Open Access Dissertation is brought to you for free and open access by the Dissertations and Theses at ScholarWorks@UMass Amherst. It has been accepted for inclusion in Doctoral Dissertations by an authorized administrator of ScholarWorks@UMass Amherst. For more information, please contact scholarworks@library.umass.edu.

**BURROWING AND WALKING MECHANISMS OF
NORTH AMERICAN MOLES**

A Dissertation Presented

by

YI-FEN LIN

Submitted to the Graduate School of the University of Massachusetts Amherst

in partial fulfillment of the requirements for the degree of

DOCTOR OF PHILOSOPHY

May 2017

Organismic and Evolutionary Biology

© Copyright by Yi-Fen Lin 2017

All Rights Reserved

**BURROWING AND WALKING MECHANISMS OF
NORTH AMERICAN MOLES**

A Dissertation Presented

by

YI-FEN LIN

Approved as to style and content by:

Elizabeth R. Dumont, Chair

Gary B. Gillis, Member

Duncan J. Irschick, Member

Brian R. Umberger, Member

Elizabeth R. Dumont, Director, Interdisciplinary
Graduate Programs

Organismic and Evolutionary Biology

DEDICATION

To my parents, who always provided love and encouragement

ACKNOWLEDGMENTS

I would like to express my deepest appreciation to my advisor, Professor Elizabeth Dumont. Without her support and patient guidance, this thesis would not have been possible. I would also like to thank my committee members, Professors Duncan Irschick, Gary Gillis and Brian Umberger for their constructive criticisms and constant encouragement. For the XROMM project, I would like to thank Professors Tom Roberts, Elizabeth Brainerd, Nicolai Konow and Angela Horner for their thoughtful planning and technical support. I would also like to thank the following funding sources that supported my work over the years: the National Science Foundation (the Doctoral Dissertation Improvement Grant), Sigma Xi (Grant-in-Aid of Research program), and the University of Massachusetts Amherst (OEB Research Grant and Natural History Collections Grant).

My graduate program, OEB has been a great community. My cohort, Andy Conith and Moira Conith, and labmates, Tom Eiting, Nina Veselka, Dan Pulaski, Brandon Hedrick and Abby Linden have given me the warmest supports and academic advice in various aspects. Behavior and Morphology Group always offered valuable suggestions that helped me refine my grant proposals and paper manuscripts. The OEB program manager, Penny Jaques, has been like a mom who made OEB like home.

Research on live moles is tough. I would like to thank friends who welcomed me for mole hunting in their yard, farms and premises: Vanna and Jimmy from the Alligator Brook Farm, Teddy's camping ground in Hadley, Amherst Golf Club, Diane Kelly, Dale Callaham, Adam and Beth, Lindsay and Barbara, Tom French, Susan Laforte and Howard Nicholson. I also want to thank the UMass IACUC members: Dr. Paul Spurlock,

Dr. Joanne Huyler, Aileen Thomas and the Animal Care Services for their tremendous help with animal husbandry. My mole team has done an amazing job helping me running experiments and data analysis. This army consists of a group of lovely UMass undergrads: Ashleen Chappuis, Shauna Rice, Chandler Burnham, Zena Casteel, Maya Gelbard, Emily Dinjian, Jessica Hien, Lauren Ramos, Erika Nevins, Sarah Bouffard, Kylie Amaral and Olivia Shiffman. Thank you all!

Last, I would not be able to complete this dissertation without the support of my husband, Yung-Chih. He is the first member of my mole team who identified the first available spot for mole hunting; he is also the last member of my team who read the first version of my thesis manuscript and gave me substantial suggestions. My Amherst host family, Lindsay and Barbara, who always gave me the warmest greetings and hospitality no matter when I visited their yard waiting for moles. Thank you all for this wonderful journey that makes Amherst my second hometown.

ABSTRACT

BURROWING AND WALKING MECHANISMS OF NORTH AMERICAN MOLES

MAY 2017

YI-FEN LIN

B.A., NATIONAL TAIWAN UNIVERSITY

M.A., NATIONAL TAIWAN UNIVERSITY

Ph.D., UNIVERSITY OF MASSACHUSETTS AMHERST

Directed by: Professor Elizabeth R. Dumont

Moles (Family Talpidae) are a classic example of extreme specialization, in their case highly derived forelimb morphologies associated with burrowing. Despite many observations of mole burrows and behaviors gathered in the field, we know very little about how and how well moles use their forelimbs to dig tunnels and to walk within the built tunnels to collect and transport food. The first chapter investigates the effect of soil compactness on two sympatric mole species under controlled laboratory conditions. My results demonstrate that increasing soil compactness impedes tunneling performance as evidenced by reduced burrowing speed, increased soil transport, shorter tunnels, shorter activity time, and less time spent burrowing continuously. Furthermore, differences in performance between the two mole species may be associated with differences in the structure and extent of their burrow systems or the morphology of their forelimbs. The second chapter investigates the kinematics of Eastern moles burrowing in loose and compact substrates. Using XROMM (X-ray Reconstruction of Moving Morphology), I found that moles move substrate dorsally using elevating strokes in loose substrates and

laterally using scratching strokes in compact substrates. They do not move the substrate caudally like most mammalian forelimb diggers. Furthermore, my results demonstrate that the combination of stereotypic movements of the shoulder joint, where the largest digging muscles are located, and flexibility in elbow and wrist joints makes moles extremely effective diggers in both loose and compact substrates. In the third chapter I test two hypotheses about forelimb movements during walking. The first is that moles move their shoulders by humeral long-axis rotation, as they do during burrowing and in walking echidnas. The second is that moles move their shoulders by flexion and extension in the horizontal plane, similar to sprawling reptiles. Surprisingly, my results reject both hypotheses and indicate that the way moles walk is different from that of all tetrapods that have been studied. The results of my dissertation open new horizons in the study of morphological, physiological, behavioral and ecological evolution of fossoriality, and may provide new ideas for the design of bio-inspired robots used for urban search and rescue.

TABLE OF CONTENTS

| | Page |
|--|------|
| ACKNOWLEDGMENTS..... | v |
| ABSTRACT..... | vii |
| LIST OF TABLES..... | xi |
| LIST OF FIGURES..... | xii |
| | |
| CHAPTER | |
| INTRODUCTION..... | 1 |
| I. THE EFFECTS OF SOIL COMPACTNESS ON THE BURROWING PERFORMANCE OF SYMPATRIC EASTERN AND HAIRY-TAILED MOLES..... | 4 |
| A. Introduction..... | 4 |
| B. Materials and methods..... | 7 |
| C. Results..... | 12 |
| D. Discussion..... | 13 |
| II. HOW MOLES DESTROY YOUR LAWN: THE FORELIMB KINEMATICS OF EASTERN MOLES IN LOOSE AND COMPACT SUBSTRATES | 18 |
| A. Introduction..... | 18 |
| B. Materials and methods..... | 20 |
| C. Results..... | 25 |
| D. Discussion..... | 27 |
| III. HOW DOES MOLE WALK? IT IS ALL THUMBS..... | 31 |
| A. Introduction..... | 31 |
| B. Materials and methods..... | 33 |

| | |
|--|----|
| C. Results..... | 36 |
| D. Discussion..... | 37 |
| CONCLUSION..... | 40 |
| APPENDICES | |
| A. TABLES ASSOCIATED WITH EACH CHAPTER..... | 43 |
| B. FIGURES ASSOCIATED WITH EACH CHAPTER..... | 49 |
| BIBLIOGRAPHY | 62 |

LIST OF TABLES

| Table | Page |
|--|------|
| 1.1. Soil compactness (kg cm ⁻²) in the field and used in experiments (mean ± s.d.)..... | 43 |
| 1.2. Burrowing performance in the soil of different compactness level..... | 44 |
| 1.3. Effects of soil compactness, species, and their interaction on burrowing performance. + indicates that body mass was used as a covariate in the model..... | 45 |
| 2.1. Stroke kinematics (value=mean ± s.e.m)..... | 46 |
| 2.2. Joint angle minimum (Min), maximum (Max) and range of motion (ROM= Max-Min) values in degrees (mean ± s.e.m)..... | 47 |
| 3.1. Stride parameters and shoulder joint movements (mean ± s.e.m) during four gait cycles for each of three individuals (12 cycles total). Rx, rotation along x- axis (abduction/adduction); Ry, rotation along y-axis (extension/flexion); Rz, rotation along z-axis (supination/pronation); ROM, range of motion (max angle – min angle)..... | 48 |

LIST OF FIGURES

| Figure | Page |
|--|------|
| 1.1. Study system. (A) Three-dimensional representation of the forelimb of an Eastern mole. (B) Geographical distributions and forelimb morphologies of Eastern moles (orange) and Hairy-tailed mole (blue). Sixth digit is marked in black..... | 49 |
| 1.2. Experimental setups. Burrowing tank and wooden rods used document the speed of burrowing (A) and tendency to burrow continuously over a long distance (C). “Mole farm” (B) used to document soil transport, tunnel construction and activity level during two-hour experiments..... | 50 |
| 1.3. Soil compactness and the depth range of tunnel systems in Eastern and Hairy-tailed moles. Soil compactness was measured at 10 cm intervals in four test pits for each species within the habitats where moles were caught. Gray bars illustrate the depth range for surface and deep tunnels observed in Eastern moles (Arton, 1936; Harvey, 1976) and Hairy-tailed moles (Eadie, 1939)..... | 51 |
| 1.4. Mole burrowing speed. (A) Burrowing speed from multiple trials of six Eastern and four Hairy-tailed moles. (B) Boxplot based on maximum burrowing speed for each individual. Horizontal line represents the median. Boxes represent the 25% and 75% quartiles. Whiskers represent the maximum and minimum values excluding outliers. Points are outliers that are more than $1.5 \times$ interquartile range (IQR) from the edge of the boxes..... | 52 |
| 1.5. Soil transport during tunnel construction. (A) The weight of moved soil divided by the body mass of the animals for each compactness level. (B) The length of tunnel built within two hours by compactness level. (C) The proportion of time and pattern that animals were active. The total active time (capital t) for each individual is listed next to each bar. (D) The total active time of two species within two hours. All differences were based on a Tukey HSD post hoc. One asterisk represents $P < 0.05$; two asterisks represent $P < 0.01$ | 53 |
| 1.6. Tendency to burrow over a long distance. Completion rate by distance. Sample size (n) indicates the sum of best four trials for 6 Eastern and 4 Hairy-tailed moles..... | 54 |

2.1. Morphological specializations of mole forelimb. (A) The comparison of forelimb skeleton (black) between fossorial mole rats and moles (re-drawn from (Gambaryan et al., 2005) and (Gambaryan et al., 2002), respectively). (B) Right forelimb skeleton of Eastern mole (*Scalopus aquaticus*). Humerus is widened and flattened. Elliptical humeral head (white cross) is posteriorly directed and articulated with scapular glenoid fossa. Profound ulna notch rotates along the axis of humeral trochlear (asterisk).....55

2.2. Two distinct burrowing behaviors of Eastern moles. Moles dig surface tunnels in loose soil to hunt for food at ground level. Surface tunnels are easily visible as branching raised dikes on the surface of the ground. In contrast, moles dig deep tunnels in compact soil to access underground nesting chambers. Since deep soil is compact and hard to be displaced, moles move this deep soil to the surface, where it can be seen as mole hills.....56

2.3. Makers and methods used for kinematic analysis. (A) and (B) show original X-ray video images of the Eastern moles from an dorsal and lateral view, respectively. Asterisk indicates the snout of mole. White crosses indicate the end of right (+) and left (+') scapula. White arrow indicates the long axis of sternum. In (C) and (D), bone models are superimposed on the X-ray frames using X-ray reconstruction of moving morphology (XROMM). Parasagittal plane (blue outline) is aligned with the long-axis of sternum. (E) Anatomical coordinate system (ACS) used to measure the trajectory of claw-tip (black sphere). The horizontal plane (green) is parallel to the ground surface. The parasagittal plane (blue) is aligned with the long-axis of the sternum over time. (F) Joint coordinate systems (JCSs) used to measure the rotations of shoulder, elbow and wrist joints. The numbers illustrate the defined joint angles in the current forelimb posture.....57

2.4. The displacements of claw-tip over a full stroke cycle. Mean (\pm s.e.m.) of translations of claw-tip for each individual during elevating and scratching strokes. The beginning of the stroke retraction occurs at 0% of the cycle. Vertical dottedlines indicate the beginning of stroke protraction. Arrows indicate the directions of the movements that would help loosening and removing soil.....58

2.5. Rotation of forelimb joints. Mean (\pm s.e.m.) of rotations of the distal bone relative to its proximal bone for each individual during elevating and scratching strokes. Distal bones (humerus, ulna and manus) rotate relative to

proximal bones (scapula, humerus and ulna) along x- (red), y- (green) and z- (blue) axes at shoulder (A), elbow (B) and wrist (C) joints. The beginning of the stroke retraction occurs at 0% of the cycle. Vertical dotted lines indicate the beginning of stroke protraction. Arrows indicate the movements that would help loosening and removing soil. The corresponding motion is shown in the right panel.....59

3.1. Humeral excursion and the orientation of the manus (hand) are different between moles and other terrestrial mammals. The ranges of humeral movements are illustrated as excursion arcs around the shoulder joint (light blue) relative to the horizontal plane in small mammals [8] and moles (this study). The manus of moles (gold) faces laterally. An enlarged sesamoid bone, sometimes called the sixth digit or false thumb, is lateral to the thumb (digit I).....60

3.2. Forelimb kinematics during walking. (A) Using a joint coordinate system to analyze humeral movements during walking. The movement of the humerus relative to scapula is described in x- (red, abduction+/adduction-), y- (green, extension+/flexion-), and z-axes (blue, supination+/pronation-). The mole's sixth digit touches the ground at 0% of the cycle and leaves the ground at the dotted line. (B) Displacements of shoulder joint (blue sphere), elbow joint (green sphere) and the sixth digit pivot (orange sphere) in the anatomical coordinate system. The x-axis of the coordinate system is aligned with the direction of walking and the y-axis with the ground. The middle panel illustrates the locations of each joint/pivot in the x- and z-axes projected onto the parasagittal plane (light orange plane in the top panel) as the animal moves along the x-axis. The locations at which the sixth digit touchdown, marking the beginning of the contact phase, are indicated by arrows. In the bottom panel, the white dotted circle represents the area of mole palm that touched the inkpad on the ground during mole walking. The bones that touched the ground are marked in black. (C) Forelimb movements in a gait cycle. The gray arcs illustrate the maximum shoulder flexion and extension. Scapula (green), humerus (red), ulna (blue) and manus (gold) are marked by different colors.60

INTRODUCTION

Fossoriality, specialization for life underground, has evolved multiple times in mammals as a strategy for foraging, avoiding predators, food storage and nesting (Nevo, 1979). Burrowing, however, is an energetically expensive behavior that involves loosening and removing soil as an animal tunnels (Alexander, 2003). Species that use burrowing as the primary mode of locomotion often have distinct morphologies, such as elongated claws, robust humeri, and long olecranon processes on the ulna (Edwards, 1937; Freeman, 1886). Although these morphological specializations have long been hypothesized to be adaptations to increase burrowing efficiency, the detailed mechanics of burrowing and how morphological specializations might facilitate burrowing performance is unclear.

Moles (Talpidae) present an excellent system for studying the kinematics and behaviors associated with burrowing. First, moles have evolved extreme forelimb morphologies that drive powerful “lateral thrusts”. The force of the lateral thrusts is equivalent to more than 30 times their own body weight (Arlton, 1936; Gambaryan et al., 2002; Skoczen, 1958). By comparison, the strongest human weight lifters can lift at most 3 times their own weight (Vickaryous and Olson, 2007). Second, unlike fossorial rodents that dig with their procumbent incisors, heads, forelimbs and hindlimbs, moles use only their forelimbs to burrow. This allows me to investigate burrowing behavior solely by examining forelimb movements. Finally, mole species exhibit a wide spectrum of fossoriality (semi-fossorial, aquatic/fossorial and fossorial; Gorman and Stone, 1990), morphological variation in the forelimb skeleton (e.g., long, intermediate and round humeri; Campbell, 1939), and geographic distribution (from southeastern Canada with

wet and loose soil to central United States with dry and compact soil; Carraway and Verts, 1991; Hallett, 1978; Hartman and Yates, 1985; Petersen and Yates, 1980; Yates and Schmidly, 1978), which makes them good for studying the relationship among burrowing morphology, biomechanics (burrowing performance) and ecology (habitat distribution).

Our current understanding of burrowing in moles is based on observations (Arlton, 1936; Dalquest and Orcutt, 1942; Gorman and Stone, 1990; Hamilton, 1931; Harvey, 1976; Hisaw, 1923; Skoczen, 1958; Yalden, 1966), comparative morphological studies (Campbell, 1939; Edwards, 1937; Freeman, 1886; Reed, 1951; Rose et al., 2013; Whidden, 2000; Yalden, 1966), and forces either measured (Arlton, 1936; Gambaryan et al., 2002; Skoczen, 1958) or calculated based on muscle anatomy (Rose et al., 2013).

Experimental data about burrowing behavior has remained elusive, in large part because of the difficulty of visualizing movement within opaque substrates. A recent technological innovation, XROMM (X-ray Reconstruction of Moving Morphology; Brainerd et al., 2010) provides a way to visualize burrowing behavior. XROMM is a 3D imaging technique that can be used to visualize and quantify movements using biplanar video radiography combined with model-based motion analysis. XROMM has been used to study the detailed kinematics of avian flight (Baier et al., 2007; Hedrick et al., 2012), jumping in frogs (Astley and Roberts, 2012; Astley and Roberts, 2014), feeding in ducks (Dawson et al., 2011), flight in bats (Konow et al., 2015), and mouth protrusion in fishes (Camp and Brainerd, 2014; Camp et al., 2015; Gidmark et al., 2012). This dissertation research demonstrates the feasibility of using XROMM to record the burrowing movements of moles.

The goal of my dissertation is to investigate the locomotor performance and kinematics of moles, and relate their behaviors to the physical aspects of the habitats they live in. First, I compare the burrowing performance and behavior of highly fossorial Eastern moles (*Scalopus aquaticus*) to the less specialized Hairy-tailed moles (*Parascalops breweri*), and test how their performance and behavior are affected by soil compactness (Chapter 1). Second, I use Eastern moles, the most specialized burrower among North American moles, to investigate how moles move their forelimbs while burrowing in loose and compact substrates (Chapter 2). Last, I compare the walking kinematics of Eastern moles to their burrowing kinematics since both burrowing and walking are significant portions of a mole's daily activities (Chapter 3). The results of this dissertation provide insight into the links among morphology, behavior and ecology of fossoriality, and a basis for future evolutionary studies.

CHAPTER I

THE EFFECTS OF SOIL COMPACTNESS ON THE BURROWING PERFORMANCE OF SYMPATRIC EASTERN AND HAIRY-TAILED MOLES

A. Introduction

Burrowing has evolved multiple times in both invertebrates and vertebrates (Alexander, 2003; Kley and Kearney, 2007), as subterranean niches provide protection from predators, a place to forage for and store food, relatively stable temperatures, and shelter from extreme weather (Nevo, 1979). Nevertheless, burrowing is energetically expensive for mammals (Ebensperger and Bozinovic, 2000; Lovegrove, 1989; Luna and Antinuchi, 2006; Seymour et al., 1998; Vleck, 1979; Zelová et al., 2010) because it involves both loosening soil and transporting it to the surface. Multiple morphological specializations have evolved to assist excavating and transporting soil. For example, some subterranean rodents use either forelimbs or chisel-like incisor teeth to break up soil, and then remove loosened soil by kicking it backwards with their hind feet (Bathyergidae, Ctenomyidae, and Octodontidae). Others turn 180° inside their tunnels and push the soil out with their forelimbs, heads, upper incisors, or chest (Spalacidae, Cricetidae, and Geomyidae; Stein, 2000; Wilson & Reeder, 2005).

Moles are one of the few specialized diggers that excavate soil using only their forelimbs without the assistance of their teeth or head. Mole humeri are robust (Campbell, 1939; Piras et al., 2012) (Fig 1.1A) and the primary muscle that moves the forelimb, the *m. teres major*, is greatly enlarged (Rose et al., 2013). The maximum force that moles can generate with their forelimbs is equivalent to more than 30 times their body weight

(Arlton, 1936; Gambaryan et al., 2002; Skoczen, 1958). In addition, the palms of moles are widened by a large sesamoid bone next the thumb (Mitgutsch et al., 2012; Sánchez-Villagra and Menke, 2005) (Fig 1.1A), which is presumed to give moles more surface area for digging, bracing, and pushing soil out of their tunnels (Gambaryan et al., 2002; Kley and Kearney, 2007).

Regardless of morphological specializations for burrowing, characteristics of the soil can influence the difficulty of constructing tunnels. In dense, compact soils, burrowers need to excavate and transport large amounts of soil per unit volume of tunnel. Among mammals, the energy cost of burrowing in cohesive, compact clay can be 9.5 times higher than that in loose, fine sand (Vleck, 1979). Loose soil is less dense but brings its own challenges. It collapses easily, making it more difficult to construct permanent tunnels. Tunnels built by ground squirrels, deer mice, and kangaroo rats are shorter and less complex in loose, sandy soil than in soils composed of cohesive clay and silt (Laundré and Reynolds, 1993). Moles are unusual in that they dig tunnels in both loose and compact soil. They build tunnel systems in loose surface soil in order to forage for invertebrates that are common at that soil depth (Edwards and Bohlen, 1996). In loose soil, moles use a lateral movement of the forelimb, the lateral stroke, to move soil aside and compress it into the walls of the tunnel (Hisaw, 1923). This reinforces the tunnel and helps keep it from collapsing. Moles also build deep tunnels in compact soil that they use for nesting. When the soil is too dense to press it into the sidewalls of a tunnel they transport it to the surface and deposit it in “mole hills”.

The interaction between morphological specializations for burrowing and substrate characteristics has been studied from the perspective of burrowing speed and

energetic expenditures (see review in Wu et al., 2015), but how animals change their burrowing behavior in response to soil characteristics and how behavioral flexibility affects the outcome of tunneling activity has not been evaluated. Moles (Talpidae) are well known for their specialized forelimbs and use of soil that ranges from loose to highly compact. In this study we evaluated the effects of soil compactness on burrowing performance in two sympatric species of moles, Eastern (*Scalopus aquaticus*) and Hairy-tailed (*Parascalops breweri*) moles (Fig 1.1B). Both species are recognized as fully or highly fossorial (Mason, 2006; Sánchez-Villagra et al., 2006), but there are differences in their morphology, behavior, and the characteristics of their burrows. Eastern moles have relatively large home ranges (10900 to 2800 m², Harvey, 1976) and build extensive tunnel systems for nesting that are up to 60 cm below the soil surface (Arlton, 1936). Eastern moles have exceptionally robust humeri (Campbell, 1939; Piras et al., 2012), large sixth digits, wide palms, and their eyes are covered with a thin layer of skin (Arlton, 1936, Fig 1.1B). Hairy-tailed moles have smaller home ranges (810 m², NatureServe (Hammerson, G.), 2008) and build fewer deep tunnels at shallower depths (25cm-45cm, Eadie, 1939). They also have slightly less robust humeri (Piras et al., 2012), somewhat smaller sixth digits and palms (Fig 1.1B), and their eyes are not covered by skin (Fig 1.1B). In addition, Hairy-tailed moles are more active above ground than Eastern moles, which are rarely seen at the surface (Fraser and Miller, 2008; Graves, 2002; Hamilton, 1939).

Based on these differences in burrow structure and forelimb morphology, we hypothesized that soil compactness affects burrowing performance in Eastern and Hairy-tailed moles to different extents. We defined five metrics of performance that reflect

tasks associated with burrowing and measured them in a laboratory setting: (1) burrowing speed (Ebensperger and Bozinovic, 2000; Lovegrove, 1989; Luna and Antinuchi, 2006; Vleck, 1979; Wu et al., 2015; Zelová et al., 2010), (2) the amount and rate of soil transport (Ebensperger and Bozinovic, 2000; Hickman and Brown, 1973), (3) the lengths of tunnels and rates at which they are constructed, (4) activity level (proportion of time spent active), and (5) the tendency to continuously burrow over a long distance. We chose these metrics because the net cost of transport (the energy spent to transport per meter distance, $J m^{-1}$) declines rapidly as transport speed increases (Full et al., 1990; Seymour et al., 1998; Taylor et al., 1970), and the total cost of burrowing is determined by the amount of substrate removed, the distance that substrates are displaced, and the amount of time that animals spend burrowing (Ebensperger and Bozinovic, 2000; Vleck, 1979; Vleck, 1981). We predicted that performance would decrease in both species as soil compactness increased but, given their differences in burrow characteristics and forelimb morphology, that Eastern moles would: (1) excavate soil faster, (2) transport more soil at a higher rate, (3) build longer tunnels at a higher rate, (4) burrow for longer periods of time, and (5) burrow for longer distances in all levels of soil compactness relative to Hairy-tailed moles.

B. Materials and methods

Six Eastern moles (body mass = 86.33 ± 8.96 g) and five Hairy-tailed moles (body mass = 48.8 ± 3.90 g) were collected in Amherst, Hadley, Deerfield, and Belchertown Massachusetts between 2013 and 2015. Eastern moles were caught on farmland and Hairy-tailed moles were caught in the lawns of local residents. The animals were housed in the animal facility of University of Massachusetts-Amherst. Each animal was housed

individually and fed twice daily (early morning and early afternoon). The ambient temperature was maintained at 20°C and the light cycle set to a 12 hour light:dark schedule. All experiments were conducted between 8 am and 12 pm as the animals were most active in the morning. The animals always began burrowing when placed on top of the soil; they did not need to be trained to burrow. All experimental procedures were approved by the University of Massachusetts Amherst Institutional Animal Care and Use Committee (#2013-0023).

We measured the range of soil compactness in the natural habitats of the animals by digging eight test pits, four in different areas in which each species was caught. Within each pit we measured the compactness of the soil five times every 10 cm depth using a pre-calibrated pocket soil penetrometer (Humboldt ®; compressive strength kg cm^{-2}) (Table 1.1).

For our experiments we defined three levels of soil compactness levels that reflect the environments in which animals exhibit different burrowing behaviors. Level 1 represents the compactness of the turf-soil interface where moles tear through grass roots in search of insects and grubs (compactness $< 1.5 \text{ kg cm}^{-2}$). Compactness Level 2 represents soil at a depth of 10 cm, where moles build surface tunnels and do most of their foraging for earthworms (Hallett, 1978; Hisaw, 1923, compactness 2 - 3 kg cm^{-2}). Compactness Level 3 emulates soil deeper than 30 cm where moles build deep tunnels for nesting and food storage (Arlton, 1936; Eadie, 1939; Harvey, 1976, compactness $> 3 \text{ kg cm}^{-2}$). We replicated these levels of compactness in the laboratory by compressing commercial topsoil (AGWAY® TopSoil) to the appropriate compactness level as measured in the field using the soil penetrometer (Table 1.1). In order to measure the

highest speed that animals are able to move through the soil, we added a new level, Compactness Level 0 (compactness $< 0.5 \text{ kg cm}^{-2}$), which we did not encounter in the field.

To evaluate burrowing speed we allowed the animals to burrow 25 cm into soil of different compactness levels in a rectangular tank that was 70 cm long, 9 cm wide, and 10 cm high (Fig 1.2A). This was wide enough for animals to burrow without touching the walls but narrow enough to keep them burrowing forward in a straight line. We chose 25 cm because it is the distance that most individuals were able to complete in a single trial. To determine when animals reached the 25 cm mark, we placed a vertical row of 2 mm diameter wooden rods at 25 cm. We considered the animals to have reached the 25 cm mark when the rods were tilted more than 30 degrees. Burrowing speed was recorded as the time that animals took to reach the 25 cm mark. Each individual was tested once at each compactness level on at least four non-consecutive days. The sequence of the compactness levels was randomized. Each test was spaced ten minutes apart, during which time the animals were held in a 26 cm long, 47.6 cm wide, and 20.3 cm high cage filled with loose soil in order to rest. The maximum speed of each individual in each compactness level was used in subsequent statistical analyses.

To measure the amount of soil animals displaced during tunnel construction, we allowed the animals to burrow for two hours in a rectangular tank that was 60 cm long, 7 cm wide, and 120 cm high (Fig 1.2B). The width of tank allowed animals to move without being constrained and allowed us to easily track the animals. Soil was added and compressed every 15 cm to compactness level 1, 2, or 3 until the tank was filled up to 105 cm, which we found through trial and error allowed the animals to build tunnels for

at least two hours without reaching the bottom of the tank. The location of animals was identified every 30 seconds during each trial. If the animals stopped moving for more than 5 minutes, we counted it as “resting”, otherwise we counted it as “active”. The total activity time was the sum of “active” points, each represents 30 seconds. This experiment was repeated with different compactness levels presented in random order. The minimum amount of time between experiments was two days. If an animal was not active for the entire 2-hour period, we re-ran the experiment after letting the animal rest a minimum of two days. The trial in which each individual built the longest tunnel was used in subsequent statistical analyses.

During these experiments we weighed the soil that the animals moved to the surface. We also calculated the amount of soil moved by animals relative to their body mass. The rates of soil transport and tunnel construction were calculated by dividing the amount of soil moved and tunnel length by activity time.

To assess the effect of soil compactness on the distance over which animals would burrow continuously, we allowed animals to burrow through the same tank used to measure burrowing speed but used its maximum length (50 cm) (Fig 1.2C). To track each animal’s progress through the tank, we placed vertical rows of 2 mm diameter wooden rods at 12.5 cm intervals, which provided four intervals. We judged an interval to be complete when the rods were tilted more than 30 degrees. We measured an animal’s tendency toward long-distance burrowing by noting how many intervals were completed. If an animal stopped moving for 30 minutes without completing all of the intervals, the remaining intervals were counted as incomplete. Each individual was tested on at least four non-consecutive days. On each testing day, each animal was tested once at each

compactness level. The best four performance trials for each individual in each compactness level were pooled to calculate an overall completion rate for each interval.

We used a generalized linear mixed model (GLMM) (*nlme* package in R (version 3.0.3; R Core Team, 2014), fitted using the restricted maximum likelihood; Zuur et al., 2009) to examine the effects of soil compactness and species on burrowing speed, soil transport, duration of activity, and tunnel construction. GLMMs are a generalization of simple linear regression models in which it is possible to include a large number of variables, fixed factors, and random factors. In the model, we assigned the speed, the amount and rate of soil transport, duration of activity, and the length and rate of tunnel construction as response variables, and soil compactness (categorical) and species (categorical) as fixed factors. For response variables that were clearly associated with body mass (e.g., amount of soil transported and rate of soil transport) we added body mass as a third fixed factor (continuous). We included ‘individual’ as a random factor in the model to account for repeated measurements of individuals in each compactness level. Since the two species might respond to soil compactness differently, the interaction between compactness and species was also included in the model. We tested for homogeneity of variance following the procedures in Zuur *et al.* (2009), and where this assumption was violated (rate of soil transport and tunnel construction), data were \log_{10} -transformed and homogeneity of variance confirmed before analyses were run. A Tukey’s honestly significant differences (HSD) test was used for *post hoc* testing where needed (Miller, 1981). For all tests α was set at 0.05.

C. Results

We found that soil compactness increases with soil depth but that soil was more compact in Eastern mole habitats than in those of Hairy-tailed moles (Fig 1.3, Table 1.1). This is especially true at the soil depth of 10 cm and 30 cm, where moles build their surface tunnels and deep tunnels, respectively.

As the soil compactness increased, burrowing speed decreased significantly (Fig 1.4, Tables 1.2 and 1.3). Both mole species penetrated the soil fastest at Compactness Level 0 and slowest at Level 3 (Table 1.2). Speed decreased most precipitously between compactness Levels 1 and 2 (Fig 1.4, Table 1.2). Neither species nor their interaction term was significantly associated with burrowing speed (Table 1.3). Contrary to our expectations, Eastern moles did not burrow faster than Hairy-tailed moles in any compactness level; the highest speed for either species was detected for Hairy-tailed moles burrowing in very loose soil (up to 53 m hr^{-1}) (Fig 1.4A).

Soil compactness has significant effects on the amount of soil transported and tunnel length (Table 1.3). Not unexpectedly, both species moved the least soil when burrowing in loose soil and more soil was transported as soil became more compact (Fig 1.5A). Tunnel length was inversely proportional to soil compactness. Both species built shorter tunnels as soil compactness increased (Fig 1.5B) but the interactions with soil compactness were different between species (Table 1.3). For Eastern moles, tunnel length did not differ significantly between soil compactness Levels 1, 2, and 3 (Tukey HSD; Level 1 versus Level 2, $P = 1.00$; Level 1 versus Level 3: $P = 0.18$), even though they transported more soil to the surface (Fig 1.5A, Table 1.2). In contrast, Hairy-tailed moles built much shorter tunnels in compactness Level 2 than in Level 1 (Tukey HSD; $P =$

0.002); tunnels in soil compactness Level 3 were the same length as those in Level 2 (Tukey HSD; $P = 0.73$). As Eastern moles built longer tunnels than Hairy-tailed moles at soil Compactness Level 2 (Tukey HSD; $P < 0.001$), they transported more soil relative to their body weight relative to Hairy-tailed moles (Tukey HSD; $P = 0.04$).

Although Eastern moles moved more soil and built longer tunnels than Hairy-tailed moles, the rates of soil transport and tunnel construction did not differ between the two species at any compactness level (Tables 1.2 and 1.3). However, Eastern moles burrowed for a longer period of time than Hairy-tailed moles (Fig 1.5C, 1.5D, Tables 1.2 and 1.3), resulting in more soil being displaced and the construction of longer tunnels. At level compactness Level 2, all Eastern moles were active for the full experimental time while Hairy-tailed moles were active for only half of the time (Table 1.2).

Eastern moles tended to burrow continuously for longer distances than Hairy-tailed moles, especially in compact soil (Fig 1.6). At Level 0, both species completed all four intervals. The completion rate of Hairy-tailed moles dropped in the third interval in compactness level 1, the second interval in compactness level 2, and the first interval in compactness level 3. In contrast, the Eastern moles almost always completed all four intervals in soil compactness levels 1 and 2. Their completion rates dropped precipitously in soil compactness level 3.

D. Discussion

Our results support the hypothesis that increasing soil compactness impedes burrowing performance as evidenced by reduced burrowing speed, increased soil transport, shorter tunnels, shorter periods of activity, and continuous burrowing over

shorter distances. Eastern moles burrowed at the same speed as Hairy-tailed moles but for longer times and distances. As a result, Eastern moles moved more soil and constructed longer tunnels in compact soil relative to Hairy-tailed moles.

Increased soil compactness can affect tunnel construction in two ways. First, because compact soil is denser than loose soil, animals need to loosen more compact soil per unit volume of tunnel than in loose soil. This is reflected in slower burrowing speed in compact relative to loose soil (Fig 1.4, Table 1.2; also see Lovegrove, 1989; Luna and Antinuchi, 2006; Zelová et al., 2010). Second, loosened soil must be removed from tunnels if the surrounding soil is compact and incompressible. Therefore, the distance that soil must be transported increases as soil becomes more compact. To reduce the distance of soil transport, pocket gophers divide their horizontal tunnels into segments punctuated with vertical tunnels through which to push soil to the surface. Naked mole rats (Jarvis and Sale, 1971) and *Octodon degus* (Ebensperger and Bozinovic, 2000) have evolved a “digging chain” behavior, in which groups of animals work in an assembly line to transport soil from the working face of the tunnel to the surface. Moles do not use either of these solutions to moving soil.

Moles are unique in using their specialized forelimbs to move loose and compact soils in different ways. When soil is loose and compressible (Compactness Level 0 and 1), Eastern and Hairy-tailed moles can penetrate it quickly (Table 1.2). The high burrowing speed of moles in loose soil is accomplished using their unique lateral stroke (Hisaw, 1923). Unlike rodents that loosen soil with their teeth or forelimbs and then move it out of the way, moles use their forelimbs to compress loose soil laterally into the walls of the tunnel, which reduces the quantity of soil that needs to be transported. This is

demonstrated by the fact that both species of moles built long tunnels in loose soil (Fig 1.5B) without transporting large amounts of soil to the ground (Fig 1.5A). This is especially true for the smaller Hairy-tailed moles, which moved less than 8 times their body weight in soil when building one-meter long tunnels at soil compactness Level 1 (Table 1.2). On the other hand, as the soil compactness increased, burrowing speed dropped dramatically (Fig 1.4, Table 1.2), and the amount of soil transported to surface increased (Fig 1.5A, Table 1.2). This indicates that the moles switched from compressing soil into the side of tunnels to transporting it to the surface (Arlton, 1936; Hisaw, 1923; Skoczen, 1958). Despite decreased burrowing speed in compact soil, Eastern moles built long tunnels regardless of the increasing demand for soil transport (Fig 1.5B). The relative wider palm of Eastern moles may assist soil transport by increasing the surface area of the hand (Gambaryan et al., 2002; Kley and Kearney, 2007). Overall, the specialized forelimb of moles are used both to compress loose soil into the side of tunnels and, if that is not possible, moving it to the surface.

The differences in the lengths of tunnels that Eastern and hairy-tailed moles built in captivity may reflect differences in their preferred habitats and foraging strategies. Eastern moles built longer tunnels than Hairy-tailed moles, especially in compact soil, and this is consistent with observations of their equally extensive tunnels in both loose (surface) soil and compact (deep) soil (Arlton, 1936; Harvey, 1976). In contrast, Hairy-tailed moles have relatively few tunnels in compact (deep) soil (Eadie, 1939). Hairy-tailed moles use shallower burrows and are known to leave their tunnels at night to forage on the surface (Graves, 2002; Hamilton, 1939), while Eastern moles forage inside their tunnel systems. These differences may be associated with the experimental finding that

Hairy-tailed moles were less active than Eastern moles in soil at Compactness Level 2 (Fig 1.5C and 1.5D), the depth of soil where earthworms are primarily distributed (Edwards and Bohlen, 1996).

Our field data suggest that Hairy-tailed moles use habitats with less compact soil compared to those of Eastern moles (Fig 1.3). The force required to compress loose soil into the side of a tunnel is lower than that required to compress compact soil, and so burrowing in loose soil may be more efficient for Hairy-tailed moles given their smaller body size and, by extension, diminished ability to generate high forces. Hairy-tailed moles may benefit from, not be restricted by, their smaller body in loose soils. This idea is supported by their high burrowing speed (Fig 1.4A) and the small amount of loose soil they moved to surface (Fig 1.5A, Table 1.2). As soil becomes more compact, larger body size or more effective ways to generate force could compensate for the need to move more soil. This idea is supported by the fact that Eastern moles spent the same amount of time actively constructing tunnels in all soil types (Fig 1.5C and 1.5D), resulting in tunnels of similar length at all compactness levels (Fig 1.5B).

In sum, the results of this study reveal that moles are able to burrow effectively in both loose and compact soil by changing their burrowing behaviors. Eastern and Hairy-tailed moles burrow at similar speeds and construct tunnels at similar rates, but they differ in the time they invest and the distance they travel while burrowing continuously. The many potential mechanisms underlying these behavioral differences (e.g. differences in forelimb morphology related to compressing and transporting soil; trade-offs between body size, force generation, and digging cost; strategies to balance energy usage (Jensen, 1986a; Jensen, 1986b)), and how these differences are related to digging metabolic rate

(Jensen, 1983; McNab, 1979) and interact with substrate characteristics may be fruitful areas for future study.

CHAPTER II

HOW MOLES DESTROY YOUR LAWN: THE FORELIMB KINEMATICS OF EASTERN MOLES IN LOOSE AND COMPACT SUBSTRATES

A. Introduction

Moles (Family Talpidae) are a classic example of extreme specialization owing to their remarkable forelimb morphologies for burrowing (Kley and Kearney, 2007). In contrast to most terrestrial mammals, the forelimbs of moles have migrated rostrally and the palms face laterally to assume a secondarily derived, sprawling posture (Fig 2.1A). Their uniquely short and wide humerus provides a large attachment area for the teres major muscle, which accounts for 75% of a mole's forelimb muscle volume (Rose et al., 2013). The ulna has an elongated olecranon process to provide mechanical advantage for the elbow extensors, and articulates with an expanded humeral trochlea that is not commonly seen among mammals (asterisk in Fig 2.1B). The tendinous flexor digitorum profundus muscle, which controls wrist movements in mammals, is unique in that it facilitates the transmission of force from the humerus to the widened palm (Rose et al., 2013; Yalden, 1966). Because of these specializations, moles are one of the most accomplished diggers among tetrapods. The tunnels built by a single individual commonly extend for hundreds of meters and sometimes over 1000 m (Arlton 1936; Hickman 1983, 1984). Moreover, moles generate digging forces that are equivalent to more than 30 times their own body weight (Arlton, 1936; Gambaryan et al., 2002).

Although the morphological specializations of mole forelimbs are well studied (Campbell, 1939; Gambaryan et al., 2002; Piras et al., 2012; Reed, 1951; Rose et al.,

2013; Yalden, 1966), little is known about how moles use their forelimbs to dig. A previous study discovered that the shape of the shoulder joint (glenoid fossa and humeral head; white cross in Fig 2.1B), as well as the surrounding tendons limit the mobility of the joint (Gambaryan et al., 2002). A similar limitation exists at the elbow joint where the ulnar notch is enlarged (asterisk in Fig 2.1B), presumably to stabilize elbow extension and flexion as the ulna articulates with humeral trochlea. Despite these potential specializations for limiting that range of forelimb joint motion, basic field and laboratory observations have shown that moles build different types of tunnels depending upon the compactness of the soil (Arlton, 1936; Hisaw, 1923; Lin et al., 2017; Skoczen, 1958). When in loose soil near the surface, moles dig tunnels that are visible as branching, raised dikes on the surface of the ground. When in compact soil deep underneath the surface, moles dig and transport soil to the surface and deposit it in mole hills (Fig 2.2). These very different types of tunnels raise the question of whether moles always dig in the same way or whether the kinematics of the forelimb changes in response to substrates of different compactness.

To date no study has examined the coordination of joints in the mole forelimb or its kinematic flexibility in response to substrate compactness. Eastern moles (*Scalopus aquaticus*) are a good species in which to study forelimb kinematics because they are one of the most specialized fossorial moles (Campbell, 1939; Sánchez-Villagra et al., 2006), are relatively common, and relatively easy to keep in captivity. With advances in X-ray technologies, we leveraged the X-ray Reconstruction of Moving Morphology (XROMM) technique to study the burrowing movements of moles in opaque substrates. We present the first evidence that the movements of moles' shoulder joints, where the muscles that

generate the highest digging forces act, are similar in loose and compact substrates, but that movements of the more distal elbow and wrist joints vary in response to substrate density.

B. Materials and methods

(a) Animals

Three Eastern moles (*Scalopus aquaticus*, 94.67 ± 10.2 grams) were captured in Hadley, Massachusetts and housed in captivity between 2013 and 2014. These animals were transported to Brown University and anesthetized for surgery prior to X-ray videographic recording (see below). For each surgery, spherical tantalum markers (0.5 to 1.0 mm diameter) were implanted in the scapula (1 marker), humerus (3-4 markers), and ulna (2 markers). Three subcutaneous markers (0.5 mm) were implanted in the medial, distal and lateral side of the palm. These locations were underneath the false thumb (*os falciforme*), at the base of the third digit, and at the base of the fifth digit, respectively. Six subcutaneous markers (0.8 mm) were implanted along the dorsal and ventral midline of the body. After surgery, moles recovered fully and resumed normal feeding and burrowing behavior within 3 days, with no discernable changes in movement or activity patterns. All husbandry and experimental procedures were approved by the Institutional Animal Care and Use Committee of UMass Amherst (#2013-0023) and Brown University (#1409000093).

(b) Data collection

We allowed animals to burrow in a 20 cm high \times 10 cm wide \times 50 cm long polycarbonate enclosure filled with couscous (Osem®, original plain). We used couscous

as an experimental substrate because the granules are similar in size and radio-opacity to each other. Since moles live in cohesive substrates like soil, we mixed couscous with water in the volume ratio 2:1 to increase the cohesion between couscous particles prior to each trial, and refer to this mixture as cohesive couscous. We consider experiments of two substrate types. To create an experimental environment of loose substrate, we filled the enclosure with cohesive couscous to 10 cm high. For the experimental environment of compact substrate, we filled the enclosure with cohesive couscous to 20 cm high and compressed it to 10 cm high. In both experiments the enclosure was covered with a polycarbonate lid to ensure the substrate compactness remained as designed and the substrate was not pushed out of the enclosure due to the mole's burrowing. The bottom of the enclosure was marked by opaque markers that were used to reference the horizontal, "ground level" plane for data analysis.

During the course of each individual's burrowing trial, we recorded biplanar X-ray videos. For each lateral and dorsoventral view, X-ray images were generated by two X-ray machines (Imaging Systems and Service) and captured by high-speed cameras (Phantom, version 10, Vision Research) recording at 90 Hz. The exposure settings were 80 kVp/160 mA for the dorsoventral view (Fig 2.3A) and 80 kVp/200 mA for the lateral view (Fig 2.3B). A calibration grid and cube were used at the beginning, middle and the end of experiments to calibrate the distortion of x-ray images using the XMALab protocol (www.xromm.org).

After all the trials were completed, animals were euthanized for Computed Tomography (CT) scans. These scans were used to build 3D mesh models of forelimbs

and implanted markers, using Mimics (version 16.0; 64-bit;) and Geomagic Studio (version 12; Geomagic).

(c) Forelimb motion analysis

Throughout this paper we refer to the forelimb movement performed by moles in loose substrates as an “elevating stroke” and that used in compact substrates as a “scratching stroke”. We chose three representative cycles of elevating strokes from each of two individuals and three representative cycles of scratching strokes from each of three individuals for analysis. Note that the numbers of individuals and trials were constrained by the availability of animals, whether individuals used their marker-implanted right hand to move substrates, and the frequency with which complete stroke cycles were captured within the calibrated field of view. For each data set we used the marker-based XROMM workflow (Brainerd et al., 2010; Gatesy et al., 2010) to construct a model and obtain forelimb kinematics.

We calibrated distorted x-ray images and digitalized markers using XMALab 1.3.3 (Knörlein et al., 2016). For bones implanted with at least 3 markers (humerus and manus), we combined marker coordinates from X-ray videos with marker coordinates from 3D bone models to calculate rigid-body transformations (Brainerd et al., 2010). For bones with fewer than three markers (scapula and ulna), we used Scientific Rotoscoping to align 3D mesh bone models to match their positions in both x-ray images (Gatesy et al., 2010).

We present two types of analysis in this study. The first type visualizes the overall movement of the whole limb over time by tracking the displacement of the claw-tip

within an anatomical coordinate system (ACS; Fig 2.3E). The second describes relative joint movements at shoulder, elbow and wrist within a series of joint coordinate systems (JCSs; Fig 2.3F)

To visualize the overall movement of the whole limb we tracked the movements of a virtual marker placed on the tip of the right 3rd claw in 3D space over time (black sphere in Fig 2.3E). The center of the ACS (0,0,0) was defined as the location of that virtual point at the beginning of a stroke. Since we were interested in the trajectory of burrowing stroke relative to the midline of the body (blue outline and plane in Fig 2.3C, 2.3D, and 2.3E) and horizontal plane of the ground (green plane in Fig 2.3E), we aligned the x-axis of the anatomical coordinate system with the long-axis of the sternum (white arrow in Fig 2.3A); the z-axis was perpendicular to the horizontal plane (green plane in Fig 2.3E). The displacements of the point along x-, y-, z-axes were then tracked, representing the movements of the whole limb in cranial (+)/caudal (-), lateral (+)/medial (-) and dorsal (+)/ventral (-) directions.

Each JCS described the movements of the distal bone relative to the proximal bone (Fig 2.3F). For shoulder and carpal joints, the center of the coordinate system (0,0,0) was defined as the middle point of the line connecting the lateral and medial sides of humeral and ulnar heads, assuming a hinge joint (Reed, 1951). For the elbow joint, a sphere was placed in the trochlear notch to approximate the center of rotation. After the $(0^\circ, 0^\circ, 0^\circ)$ was determined, we aligned orthogonal axes with the anatomical axes of the distal bone, first by determining the long axis of the bone (z-axis; supination (+) /pronation (-)), and then oriented the craniocaudal (y-axis; extension (+) /flexion (-)) and dorsoventral axis (x-axis; abduction (+) /adduction (-)) (Pierce et al., 2012). For the

shoulder, elbow and wrist joint, the craniocaudal axis was parallel to the humeral plane, perpendicular to ulna plane and parallel to the plane of manus, respectively (green y-axis, Fig 2.3F). After the center and axes of each JCS was determined, we defined a reference angle for each JCS at each joint to describe joint movements relative to a neutral position. For shoulder, when humeral plane is perpendicular to the long-axis of scapula and its long-axis is parallel to glenoid fossa, the XYZ angle of humerus relative to scapula is (0° , 90° , 90°), respectively. For elbow, when ulna has its long-axis perpendicular to humeral plane and its craniocaudal axis parallel to trochlear fossa, the XYZ angle of ulna relative to humerus is (0° , 90° , 90°), respectively. For wrist, when the plane of manus bone is parallel to the plane of ulna head and its craniocaudal axis is parallel to the line connecting the two protruding ends of ulnar head, the XYZ angle of manus relative to ulna is (0° , 0° , 0°), respectively (Fig 2.3F).

We analyzed the XYZ displacement of the stroke trajectories and angular joint motions with the same procedures. Data points over one full stroke cycle were normalized to 101 points (corresponding to 0-100% of a stroke cycle) using cubic spline interpolation (O'Neill et al., 2015). This allowed us to calculate the mean and standard error of the mean of kinematic curves for each individual in each substrate. The beginning of forelimb retraction was defined as the moment at which an animal's forelimbs were closest to each other in front of its head. The beginning of forelimb protraction was defined as the moment at which an animal's forelimbs were most separated from each other at the sides of body. We then calculated the durations of retraction and protraction within each cycle. We defined stroke velocity as the

displacement of claw-tip trajectory per second (cm/s) in 3D space, and stroke frequency as the inverse of stroke duration.

C. Results

Stereo x-ray kinematics measurements on the trajectory of the claw-tip revealed that moles moved their whole limbs in very different directions during elevating and scratching strokes (Fig 2.4). During the retraction phase of the elevating stroke, the claw-tip moved primarily along the dorso-ventral (z) axis, and one individual also moved its claw along the medio-lateral (y) axis, indicating that the whole limb moved vertically from ventral to dorsal and, in one individual, laterally. In contrast, during the retraction phase of the scratching stroke, the claw-tip moved primarily laterally (y-axis) and, to a lesser extent, cranio-caudally (x-axis). Elevating strokes were executed with lower velocity (13.83 ± 1.16 cm/s) and frequency (1.91 ± 0.14 times/sec) compared to scratching strokes (21.21 ± 1.22 cm/s; 3.39 ± 0.17 time/sec) (Table 2.1).

Kinematics analysis of joint movements revealed that substantial humeral long-axis pronation and flexion are the primary movements of the shoulder during elevating and scratching strokes (Fig 2.5A). There was a similar degree of shoulder flexion between elevating and scratching strokes, but the range of pronation was greater during scratching than during elevating strokes (Table 2.2). In addition, during scratching strokes humeral pronation and flexion continued until the end of retraction. In contrast, during elevating strokes both rotations stopped earlier and the plane of the humerus was nearly perpendicular to the long-axis of the scapula until the end of retraction.

In both elevating and scratching strokes elbow extension started at the beginning of retraction, followed by elbow adduction. However, the elbow motion during the two strokes differed at the end of forelimb retraction. During scratching strokes the elbow continued adducting until the end of retraction. In contrast, during elevating strokes the elbow adducted with a smaller range relative to scratching strokes but performed a secondary elbow extension before the end of the retraction phase (Fig 2.5B).

Elevating and scratching strokes exhibited opposite patterns of movement at the wrist. During scratching strokes, the wrist flexed and subsequently adducted and pronated till the end of retraction. In contrast, adduction and pronation happened first during elevating strokes and were followed by wrist flexion. In both elevating and scratching strokes, the timing of wrist flexion coincided with the point at which moles encountered challenges such as compressing soil to the wall or breaking compact soil. In contrast, the timing of wrist adduction and pronation was synchronized with the timing when moles moved loose or loosened substrates.

In sum, the movements of the limb during elevating and scratching strokes were very different and associated with different patterns of joint movement. In loose substrates, moles used elevating strokes to move the substrate dorsally and laterally. This movement started with humeral pronation, humeral flexion and elbow extension, and was followed by a secondary elbow extension and wrist flexion at the end of retraction. These latter movements served to compress the substrate to open a tunnel. In contrast, moles used scratching strokes to advance a tunnel in compact soil. Scratching strokes started with the same joint motions as elevating strokes, but these movements were followed by

elbow adduction, wrist adduction, and wrist pronation, which served to sweep soil laterally before it was transported to the surface.

D. Discussion

Moles exhibit unique stroke trajectories and soil displacement mechanisms relative to other mammalian forelimb diggers. Most fossorial mammals use scratching or hook-and-pull digging primarily in a parasagittal plane to move substrate caudally when digging (B. Campbell 1938; Reed 1951; Gasc et al. 1986; Hildebrand 1985a; Kley and Kearney, 2007). In contrast, moles have evolved rostrally-migrated and hyper-abducted forelimbs, and move substrates perpendicular to the midlines of their upper bodies during forelimb retraction. This unique movement allows moles to construct tunnels efficiently near the surface where the soil is relatively loose (Chapter 1, Lin et al., 2017) and prey are abundant (Edwards and Bohlen, 1996). When burrowing in this type of substrate, moles use a single elevating stroke to move soil and compress it into the side of the tunnel. This efficient, single stroke allows moles to move quickly through loose soil and build tunnels for foraging. On the other hand, when burrowing in compact substrates that are usually deep in the ground and difficult to displace (Lin et al., 2017), moles advance a tunnel by scratching the soil laterally (Fig 2.4) and then transporting it out of the tunnels. To move soil out of tunnels, moles use their hindlimbs to kick soil backward or twist their upper body to one side during scratching strokes to direct soil more directly behind them (Arlton, 1936; Hisaw, 1923; Skoczen, 1958). Although scratching strokes require these additional movements to remove soil, moles complete one scratching stroke much faster than an elevating stroke.

With respect to joint movements, we found that movement at the shoulder joint is similar during elevating and scratching strokes but that movements of the more distal elbow and wrist joints differ substantially. Therefore, it is critical to understand the movements at each joint.

Most of the force of mole digging is assumed to be generated by muscles surrounding the shoulder joint (Gambaryan et al., 2002; Rose et al., 2013). In eastern moles, the teres major muscle accounts for 75% of total forelimb muscle volume and so generates a large proportion of forelimb muscle force while it contracts (Gambaryan et al., 2002; Rose et al., 2013). The contractions of teres major, together with latissimus dorsi, subscapularis and pectoralis superficialis posticus, result in humeral pronation and flexion (Reed, 1951, Yalden, 1966, Hildebrand 1982, 1985a, Gambaryan et al., 2002, Rose 2013). These two humeral movements were both observed at the beginning of both elevating and scratching strokes, showing the centrality of shoulder movements in both loose and compact substrates. We also documented that the humeral plane remains nearly perpendicular to the long-axis of the scapula when moles use elevating strokes to compress the substrate at the end of limb retraction. This particular position provides teres major the highest moment arm to generate input torque along the shoulder joint (Gambaryan et al., 2002). Our findings, along with those of some previous studies, suggest that moles are efficient burrowers and argue against other studies that suggested that the humeral plane is parallel to the parasagittal plane at the end of retraction (e.g., Todorowa, 1927; Reed, 1951; Yalden, 1955).

Unlike shoulder movements, the elbow movements are different between elevating and scratching strokes at the late stage of forelimb retraction. At the end of the

retraction phase of the elevating stroke, moles employed a secondary elbow extension to compress the substrate into the wall of the tunnel. This reinforces the tunnel wall using a single stroke. In contrast, moles use elbow adduction during scratching strokes to sweep soil in both lateral and caudal directions. This movement also helps moles to avoid the increased moment arm of the ground reaction force at the elbow joint when the elbow extends (Gambaryan et al., 2002). This adduction and sweeping motion is reinforced by an expanded humeral trochlea and enlarged humeral epicondyles that prevent elbow dislocation during elbow adduction (Gambaryan et al., 2002).

Moles use different wrist movements when moving loose and compact substrates. When compressing or breaking apart the substrate, moles use wrist flexion. On the other hand, when moving loose or loosened substrates, the wrist is adducted and pronated. We hypothesize that wrist flexion assists compressing or breaking apart substrates by imposing a force that is perpendicular to the surface of the substrate, whereas wrist adduction and pronation facilitate sweeping the substrate by covering more ground area in one stroke.

Researchers have long speculated about the joint motion and burrowing mechanisms of fossorial tetrapods based on the morphological specializations of their forelimbs. Although frequently invoked, the connection between these morphological specializations and the associated joint movements during burrowing is seldom tested. Here, we present the first unequivocal evidence of how moles coordinate their specialized forelimb joints to dig in response to the changes in substrate compactness. The results of this study argue against previous hypotheses about moles' stroke trajectories and the motion of shoulder and elbow joints, and provide novel insights into the joint motion

associated with their unique morphologies and kinematic flexibility. This study expands our understanding of burrowing biomechanics and may have implications for bio-inspired designs for burrowing.

CHAPTER III

HOW DO MOLES WALK? IT IS ALL THUMBS

A. Introduction

Mammalian ancestors had a sprawling posture with limbs extending to the side, and the migration of the limbs underneath the body to produce an upright stance is a hallmark of mammal evolution (Bakker, 1971; Biewener, 1990; Crompton and Jenkins, F. A., 1973). Erect posture is one of many transitions associated with energy savings that evolved in concert with the ever-increasing metabolic demands of early mammals; it confers energy savings by supporting body weight directly along the long axes of limb bones rather than wasting mechanical energy on contraction of limb extensors (Biewener, 1989). It also allowed them to be less constrained by the substrates they interacted with and, by reducing the lateral undulation associated with a sprawling gait, to move faster (Bakker, 1971; Heglund et al., 1982). Despite the apparent advantages of an upright stance, a secondarily derived, sprawling posture has evolved in a few mammals that have unique locomotor niches. These include semi-aquatic species that use the limbs to swim (e.g., seals, sea lions, walrus, and otters) and moles that live their lives almost completely underground.

Moles (Family Talpidae) are among the most specialized fossorial mammals and exhibit the most exaggerated sprawling stance (Fig 3.1). Their short, broad humerus is oriented dorsally (toward the back) and anteriorly (toward the nose), and their palm, which is significantly widened by a “false thumb” (*os falciforme* or sixth digit), faces to the side and away from the body (Fig 3.1). With this forelimb anatomy and posture,

moles can compress loose soil into the walls of their tunnels (Chapter 2) instead of transporting it the surface (Chapter 1, Lin et al., 2017) at the expense of metabolic energy (Vleck, 1979). Individual Eastern moles occupy home ranges exceeding 10,000 m² (Harvey, 1976) and 23-42 times larger than those of fossorial pocket gophers (Yates and Schmidly, 1978). Eastern moles patrol their tunnels over 400 m/day to forage and transport food (Harvey, 1976). Walking is thus a significant portion of a mole's daily activities. A recent kinematic study revealed how the mole forelimb moves during burrowing (Chapter 2), yet it remains unknown how moles use their highly specialized forelimbs during walking.

In this study we use X-ray Reconstruction of Moving Morphology (XROMM) to study mole forelimb kinematics during walking. We test two hypotheses about limb movements at the shoulder joint. The first is that the main movement at the shoulder is humeral long-axis rotation, which is the main driver of mole burrowing movements (Reed, 1951) and of walking in echidnas (Jenkins, 1970; Jenkins, 1971). The second hypothesis is that the primary movement at the shoulder joint is flexion/extension in the horizontal plane, as seen in reptiles with sprawling postures (Baier and Gatesy, 2013; Gambaryan, 2002; Jenkins and Goslow, 1983). We also characterize the position of the shoulder, elbow, and 6th digit relative to one another across the contact and swing phases of the walking gait cycle to determine their degree of similarity with respect to those of other tetrapods.

B. Materials and methods

(a) Animals

We captured three Eastern moles (*Scalopus aquaticus*, 94.7 ± 10.2 g) in Hadley, Massachusetts and housed them in captivity between 2013 and 2014. All husbandry and experimental procedures were approved by the Institutional Animal Care and Use Committee of UMass Amherst (#2013-0023) and Brown University (#1409000093). We transported these animals to Brown University and anesthetized them for surgery prior to X-ray video graphic recording (see below). During sterile surgery we implanted one 1mm spherical tantalum marker in the right scapula, three to four 0.5mm markers in the right humerus, and two 0.5-1mm markers in the right ulna. We also implanted three 0.5mm subcutaneous markers in the palm underneath the false thumb (*os falciforme*, medial), at the base of the third digit (distal), and at the base of the fifth digit (lateral). After surgery, moles recovered fully and resumed normal feeding and burrowing behavior within three days. There was no discernable difference in their movements or activity patterns pre- and post-surgery.

(b) Data collection

Animals were allowed to voluntarily walk in a 20 cm high \times 7 cm wide \times 50 cm long radio translucent polycarbonate enclosure. Before surgery the moles walked across a non-toxic inkpad so that we could visualize which parts of their hands contacted the ground. To understand which bones contact the ground and the movement of the forelimb, we recorded biplanar x-ray videos of moles with implanted markers walking, after they recovered from surgery. For this experiment, the enclosure was marked using radio-opaque markers to reference the “ground level” for analyses. For each lateral and

dorsoventral view, X-ray images were generated by two X-ray machines (Imaging Systems and Service; 55 kVp/250 mA) and captured by high-speed cameras (Phantom, v10, Vision Research) recording at 90 Hz. A calibration grid and cube were filmed at the beginning, middle and the end of experiments to calibrate the distortion of x-ray images using the XMALab protocol (www.xromm.org).

After completion of the walking trials, animals were euthanized for Computed Tomography (CT) scanning. The scans were used to build 3-D models of the forelimb skeletal elements (scapula, humerus, ulna, and manus) and implanted markers using Mimics (version 16.0) and Geomagic Studio (version 12; Geomagic).

(c) Forelimb motion analysis

We chose four consecutive cycles of walking from each of three individuals for the analysis. We used the marker-based XROMM workflow (Brainerd et al., 2010; Gatesy et al., 2010) to construct a digital model and calculate forelimb joint kinematics. We calibrated distorted x-ray images and digitized markers using XMALab 1.3.3 (Knörlein et al., 2016). For bones implanted with at least 3 markers (humerus and manus), we combined marker coordinates from X-ray videos with marker coordinates from 3D models of the bones to calculate rigid-body transformations (Brainerd et al., 2010). For bones with fewer than three markers (scapula and ulna), we used Scientific Rotoscoping to align 3D models of bones to match their positions in both x-ray images (Gatesy et al., 2010).

Here, we present two analyses. The first describes relative movements at the shoulder joint within a joint coordinate system (Fig 3.2A). The second visualizes the

trajectories of the shoulder joint, elbow joint and sixth digit over time by tracking their displacements within an anatomical coordinate system (Fig 3.2B).

The joint coordinate system described the movements of the humerus relative to the scapula (Fig 3.2A). The origin of the coordinate system (0,0,0) was defined as the middle point of a line connecting the two sides of the humeral head, assuming that it acted as a hinge joint (Reed, 1951). After determining the origin (0,0,0), we aligned the z-axis with the long axis of the humerus (supination (+) /pronation (-)) and the y-axis parallel with the plane through the width of the relatively flat humerus (humeral plane; extension (+) /flexion (-)) (Fig 3.2A, top panel). We then defined a reference angle for the joint coordinate system in order to describe joint movements relative to a neutral position. For the shoulder, when the humeral plane is perpendicular to the long-axis of the scapula and its long-axis is parallel to the glenoid fossa, the XYZ angle of humerus relative to scapula is (0 °, 90°, 90°, Fig 3.2A, top panel).

To visualize the relative locations of the shoulder joint, elbow joint and sixth digit (blue, green, and orange spheres in Fig 3.2B, respectively), we tracked their displacements in 3D space over time. The origin of the anatomical coordinate system (0,0,0) was defined as the location of the sixth digit at the beginning of contact phase in the first gait cycle. We were interested in the trajectory of the joints and sixth digit relative to the ground and the direction of movement of the animal. Therefore, we aligned the x-axis of the anatomical coordinate system with a line that passed through each point at which the sixth digit first contacted the ground (small orange spheres in Fig 3.2B); the z-axis was perpendicular to the horizontal plane (i.e., vertical). The displacements of joint centers and the sixth digit along x-, y-, z-axes were tracked to illustrate their movements

in cranial (+) and caudal (-) (x-axis), lateral (+) and medial (-) (y-axis), and dorsal (+) and ventral (-) (z-axis) directions.

The 6th digit was always the first and last to contact the ground and so was used to define the contact and swing phases of the gait cycle. We analyzed the angular movement of the shoulder joint and XYZ displacement of the shoulder and elbow joint centers and the sixth digit by normalizing data over each gait cycle to 101 points (corresponding to 0-100% of a stroke cycle) using cubic spline interpolation (O'Neill et al., 2015). This allowed us to calculate mean values and standard errors for kinematic curves for each individual. We calculated the durations of contact and swing phases within each gait cycle as well as the duty factor (percentage of the stride where the forelimb touches the ground). We defined walking speed as the 3-D displacement of the sixth digit per second (cm/s), and stride frequency as the inverse of stride duration.

C. Results

Moles walked at a speed of 18.4 ± 2.0 cm/s with a duty factor of 0.56 ± 0.02 (Table 3.1). The average range of excursion of the long-axis of the humerus was 125 - 155° relative to the horizontal plane and -1 - 17° relative to the parasagittal plane (these values are expressed as excursion arcs in Fig 3.1). The movement of the humerus above the horizontal plane (Fig 3.1, top right) and in the parasagittal plane (Fig 3.1, bottom right) is unique among all tetrapods studied to date.

During swing phase, moles performed humeral extension to increase stride length (Fig 3.2A). Maximum humeral extension occurred before the sixth digit contacted the ground (Fig 3.2C). This contradicts the hypothesis that moles move their shoulder by

humeral long-axis rotation when they walk, as they do when they burrow or as echidnas do when they walk.

During contact phase, the sixth digit was always in front of the shoulder and elbow joints (Fig 3.2B, middle panel). This is fundamentally different from other terrestrial tetrapods in which the manus lags behind the shoulder and elbow joints during the contact phase. The sixth digit and thumb were the only portions of the palm that touched the ground during walking (Fig 3.2B, bottom panel). The sixth digit touched the ground first, followed by the thumb, together forming a stable support.

D. Discussion

Our results demonstrate that the movement of the mole forelimb during walking is unique relative to the forelimbs of echidnas (Jenkins, 1970) and reptiles with a sprawling posture (Baier and Gatesy, 2013; Gambaryan, 2002; Jenkins and Goslow, 1983), as well as other terrestrial mammals, including those specialized for running (Bakker, 1971; Charig, 1972; Gregory, 1912; Jenkins, 1971; Kardong, 1995). Like sprawling reptiles and terrestrial mammals, the mole shoulder joint flexes and extends during walking, but it happens above rather than below the horizontal plane (Baier and Gatesy, 2013; Gambaryan, 2002; Jenkins and Goslow, 1983). The extension and flexion of the shoulder during walking differs substantially from burrowing, where long-axis rotation is the primary movement (Chapter 2). It may be that walking requires less muscle force than burrowing and so the shoulder muscles may be able to stretch beyond the optimal length for force generation. This opportunity for the shoulder muscles to stretch may permit the shoulder extension associated with the walking stride. The difference in forelimb

movement between moles and echidnas could be linked to the fundamentally different gaits used by two species. Echidnas walk with a pace-like gait, moving both fore and hindlimb on either side together, resulting in a noticeable side-to-side (yaw) motion of the trunk (Gambaryan and Kuznetsov, 2013). Our observations reveal a symmetrical gait in moles with diagonal limbs contacting the ground synchronously and less exaggerated lateral body undulation that are typical of tetrapod walking. The mechanisms underlying the differences between moles and echidnas, such as the differences in joint morphologies and muscle-tendon architectures, will require further investigation.

Moles walk at speeds similar to “high walking” alligators, geckos, skinks, and similarly-sized ground squirrels and chipmunks (10-20 cm/s, Biewener, 1983; Biewener, 2006; Farley and Ko, 1997; Willey et al., 2004). However, they have a much lower duty factor (0.56 compared to 0.7-0.9, Biewener, 1983; Biewener, 2006; Farley and Ko, 1997; Willey et al., 2004), approaching the cut-off (<0.5, Biewener, 2006) defining running. When moles walk, only the thumb and 6th digit on the medial side of the palm touch the ground during contact phase. It is possible that the 6th digit, a sesamoid bone, functions to support the mole’s body weight much as the radial sesamoid bone of elephants bears body weight when animals change foot posture (Hutchinson et al., 2011; Panagiotopoulou et al., 2016). A mole’s sixth digit and thumb are always in front of the shoulder and elbow joints. This is similar to the way that people use walking canes. The cane (or 6th digit) is placed on the ground in front of the body, which then moves forward to meet it. This form of gait appears to be unique among tetrapods, in which the distal forelimb element (hoof, pad or palm) is far behind the shoulder by the end of contact phase (Baier et al., 2013; Gambaryan, 2002; Gambaryan et al., 2002; Jenkins, 1970;

Jenkins and Goslow, 1983). The fact that moles do not extend the contact phase by allowing the shoulder to move forward of the hand may be linked to the relatively low duty factor. We do not know whether moles use their strong forelimbs to generate propulsion during walking, like vampire bats (Riskin and Hermanson, 2005), or use their hind limbs like generalized tetrapods (Heglund et al., 1982).

The results of this study increase our understanding of the breadth of tetrapod limb posture and locomotion, highlight the need to examine the influences of joint morphologies on joint mobility (Pierce et al., 2012; Pierce et al., 2013), and demonstrate the importance of advanced x-ray techniques in revealing hidden movements during tetrapod locomotion.

CONCLUSION

Moles (Family Talpidae) are a classic example of extreme specialization, in their case highly derived forelimb morphologies associated with burrowing. Despite many observations of mole burrows and behaviors gathered in the field, we know very little about how and how well moles use their forelimbs to dig tunnels in loose and compact soils, and to walk within the built tunnels to collect and transport food. The first chapter documents that increasing soil compactness impedes tunneling performance as evidenced by reduced burrowing speed, increased soil transport, shorter tunnels, shorter activity time, and less time spent burrowing continuously. Eastern moles built longer tunnels than hairy-tailed moles as soil compactness increased. This difference is linked to burrowing for longer times and distances, not higher burrowing speeds or rates of soil transport. Differences in performance between the two species may be associated with differences in the structure and extent of their burrow systems or the morphology of their forelimbs. They may also reflect preferences for loose (Hairy-tailed moles) or compact soils (Eastern moles). The second chapter investigates the kinematics of Eastern moles burrowing in loose and compact substrates. Using XROMM (X-ray Reconstruction of Moving Morphology), I found that moles move substrate dorsally using elevating strokes in loose substrates and laterally using scratching strokes in compact substrates. They do not move the substrate caudally like most mammalian forelimb diggers. Both elevating and scratching strokes are characterized by similar ranges of humeral pronation and flexion, but the movements of the elbow and wrist differ. Eastern moles extend the elbow and flex the wrist during elevating strokes to compress soil into the tunnel wall. During scratching strokes they adduct the elbow and both adduct and pronate the wrist to sweep

soil laterally before transporting it to the surface. My results demonstrate that the combination of stereotypic movements of the shoulder joint, where the largest digging muscles are located, and flexibility in elbow and wrist joints makes moles extremely effective diggers in both loose and compact substrates. In the third chapter I test two hypotheses about forelimb movements during walking. The first is that moles move their shoulders by humeral long-axis rotation, as they do during burrowing and in walking echidnas. The second is that moles move their shoulders by flexion and extension in the horizontal plane, similar to sprawling reptiles. Surprisingly, my results reject both hypotheses and indicate that the way moles walk is different from that of all tetrapods that have been studied. Like sprawling reptiles and most terrestrial mammals, the mole shoulder joint flexes and extends during walking, but it happens above rather than in or below the horizontal plane. They also appear to use the radial sesamoid bone in the palm (also known as the sixth digit or false thumb) to support their body weight during the contact phase of the gait cycle. When moles walk, the sixth digit and thumb are always in front of the shoulder and elbow joints. This form of gait appears to be unique among tetrapods, in which the distal forelimb element (hoof, pad or palm) is far behind the shoulder by the end of contact phase. This study increases our understanding of the breadth of tetrapod limb posture and locomotion, highlights the need to examine the influences of joint morphologies on joint mobility, and demonstrates the importance of advanced x-ray techniques in revealing hidden movements during tetrapod locomotion. In sum, my dissertation reveals that moles are able to burrow effectively in both loose and compact soil by changing their burrowing behaviors and kinematics. The forelimb morphological specializations for burrowing and walking render them among the most

accomplished fossorial tetrapods. The results of my dissertation open new horizons in the study of morphological, physiological, behavioral and ecological evolution of fossoriality, and may provide new ideas for the design of bio-inspired robots used for urban search and rescue.

APPENDIX A

TABLES ASSOCIATED WITH EACH CHAPTER

Table 1.1. Soil compactness (kg cm^{-2}) in the field and used in experiments (mean \pm s.d.)

| Natural habitats | Turf-soil interface | Surface tunnel | - | Deep tunnel | Deep tunnel | Deep tunnel | Deep tunnel |
|--------------------|------------------------|-------------------|-----------------|-----------------|-----------------|-----------------|-----------------|
| | 0cm | 10cm | 20cm | 30cm | 40cm | 50cm | 60cm |
| Eastern (N=4) | 0.87 \pm 0.02 | 2.59 \pm 0.08 | 3.39 \pm 0.49 | 4.13 \pm 0.20 | 3.87 \pm 0.47 | 3.78 \pm 0.54 | 3.26 \pm 0.52 |
| Hairy-tailed (N=4) | 1.08 \pm 0.61 | 2.11 \pm 0.15 | 2.4 \pm 0.43 | 2.91 \pm 0.55 | 3.37 \pm 0.26 | 3.3 \pm 0.97 | 2.94 \pm 0.50 |
| Experiments | Level 1 | Level 2 | - | Level 3 | - | - | - |
| Eastern (N=5) | 1.15 \pm 0.31 | 2.47 \pm 0.20 | - | 3.47 \pm 0.56 | - | - | - |
| Hairy-tailed (N=5) | 1.02 \pm 0.13 | 2.55 \pm 0.29 | - | 3.07 \pm 0.55 | - | - | - |

Table 1.2. Burrowing performance in the soil of different compactness level.

| Variables | Species | Compactness level | | | |
|--|--------------------|-------------------|------------|-------------|-------------|
| | | 0 | 1 | 2 | 3 |
| Maximal speed (m hr ⁻¹) | Eastern (N=6) | 28.68±7.84 | 14.95±9.06 | 2.28±0.36 | 1.02±0.70 |
| | Hairy-tailed (N=4) | 36.68±15.79 | 15.84±8.29 | 2.57±0.93 | 1.28±0.55 |
| Total amount of soil transported (g) | Eastern (N=5) | - | 1934±630 | 3216±319 | 3683±553 |
| | Hairy-tailed (N=5) | - | 397±234 | 656±434 | 1608±863 |
| Total soil transported (relative to body mass) | Eastern (N=5) | - | 21.69±9.85 | 42.01±5.03 | 47.40±9.52 |
| | Hairy-tailed (N=5) | - | 7.49±3.64 | 12.43±7.11 | 31.58±17.65 |
| Total tunnel length (m) | Eastern (N=5) | - | 1.25±0.25 | 1.28±0.17 | 0.87±0.21 |
| | Hairy-tailed (N=5) | - | 1.12±0.41 | 0.43±0.19 | 0.65±0.29 |
| Total active time (hr) | Eastern (N=5) | - | 1.71±0.65 | 2±0 | 1.78±0.5 |
| | Hairy-tailed (N=5) | - | 1.36±0.48 | 0.88±0.78 | 1.11±0.68 |
| Rate of soil transport (relative to body mass hr ⁻¹) | Eastern (N=5) | - | 13.21±3.74 | 21.01±2.52 | 30.76±18.62 |
| | Hairy-tailed (N=5) | - | 6.50±4.19 | 34.83±36.41 | 31.26±15.33 |
| Rate of tunnel construction (m hr ⁻¹) | Eastern (N=5) | - | 0.88±0.52 | 0.64±0.08 | 0.53±0.22 |
| | Hairy-tailed (N=5) | - | 0.96±0.53 | 1.40±1.64 | 0.74±0.57 |

Table 1.3. Effects of soil compactness, species, and their interaction on burrowing performance. ⁺ indicates that body mass was used as a covariate in the model.

| Variables | Soil compactness | | Species | | Soil compactness × Species | |
|---|-------------------------|-------------------|------------------------|-------------------|----------------------------|-----------------|
| | F | P-value | F | P-value | F | P-value |
| Maximal speed (m hr ⁻¹) | 37.61 _[3,23] | < .0001*** | 0.62 _[1,8] | 0.45 | 0.98 _[3,23] | 0.42 |
| Total soil transport ⁺ (g) | 16.77 _[2,10] | 0.0006*** | 62.00 _[1,8] | < .0001*** | 1.77 _[2,10] | 0.22 |
| Total tunnel length (m) | 9.07 _[2,16] | 0.0023** | 16.32 _[1,8] | 0.0037** | 6.93 _[2,16] | 0.0068** |
| Total active time (hr) | 0.10 _[2,16] | 0.91 | 8.32 _[1,8] | 0.02* | 1.42 _[2,16] | 0.27 |
| Rate of soil transport ⁺ (g hr ⁻¹) | 87.79 _[2,10] | < .0001*** | 0.89 _[1,8] | 0.37 | 10.0 _[2,10] | 0.004* |
| Rate of tunnel construction (m hr ⁻¹) | 1.62 _[2,16] | 0.23 | 0.13 _[1,8] | 0.73 | 0.07 _[2,16] | 0.94 |

Table 2.1. Stroke kinematics (value=mean±s.e.m)

| | Displacement (cm) | | Duration (sec) | | Velocity (cm/s) | | Stroke Frequency (Hz) | Stroke Velocity (cm/s) |
|----|-------------------|-----------|----------------|-----------|-----------------|------------|-----------------------|------------------------|
| | Retract | Protract | Retract | Protract | Retract | Protract | | |
| ES | 3.22±0.08 | 4.02±0.27 | 0.36±0.03 | 0.18±0.03 | 9.35±0.75 | 24.05±3.45 | 1.91±0.14 | 13.83±1.16 |
| SS | 3.65±0.18 | 2.70±0.31 | 0.20±0.01 | 0.10±0.01 | 18.46±0.84 | 26.72±2.81 | 3.39±0.17 | 21.21±1.22 |

ES: Elevating stroke, trials = 3 strokes from each of 2 individuals (total 6 strokes)

SS: Scratching stroke, trials=3 stroked from each of 3 individuals (total 9 strokes)

Table 2.2. Joint angle minimum (Min), maximum (Max) and range of motion (ROM=Max-Min) values in degrees (mean±s.e.m)

| | | | Shoulder | | | Elbow | | | Wrist | | |
|-------------------|----|-----|----------|---------|---------|---------|----------|---------|---------|--------|---------|
| | | | Rx | Ry | Rz | Rx | Ry | Rz | Rx | Ry | Rz |
| Stroke retraction | ES | Min | -10.5±6 | 65.1±2 | 80.1±3 | -7.6±3 | 88.1±3 | 88.8±2 | -39.9±2 | 8.8±3 | -25.7±3 |
| | | Max | 15.0±6 | 105.0±3 | 114.6±4 | 9.3±3 | 106.4±3 | 104.4±3 | -30.5±2 | 26.5±3 | -6.1±4 |
| | | ROM | 25.5±7 | 40.0±3 | 34.5±4 | 16.9±3 | 18.3±2.9 | 15.6±2 | 9.4±2 | 17.8±1 | 19.6±2 |
| | SS | Min | -11.0±5 | 42.3±4 | 60.0±4 | -21.1±4 | 78.4±2 | 88.5±1 | -31.5±3 | 0.3±4 | -14.2±5 |
| | | Max | 17.2±4 | 81.0±6 | 115.6±4 | 1.9±1 | 104.4±3 | 102.9±2 | -20.9±2 | 24.4±2 | 2.6±5 |
| | | ROM | 28.2±4 | 38.6±4 | 55.5±5 | 23.0±4 | 26.0±3 | 14.4±2 | 10.5±2 | 24.1±3 | 16.8±2 |
| Entire stroke | ES | Min | -21.4±5 | 55.3±5 | 80.1±3 | -9.8±2 | 67.1±2 | 88.6±1 | -53.4±5 | 8.4±3 | -39.8±6 |
| | | Max | 15.9±5 | 107.1±3 | 135.3±5 | 16.6±1 | 106.4±3 | 109.0±2 | -26.9±2 | 40.9±1 | -3.5±5 |
| | | ROM | 37.4±9 | 51.8±5 | 55.2±2 | 26.3±2 | 39.3±3 | 20.4±2 | 26.5±3 | 32.4±4 | 36.3±3 |
| | SS | Min | -17.1±6 | 39.0±4 | 60.0±4 | -21.1±4 | 68.1±2 | 88.5±1 | -41.1±4 | 0.2±4 | -25.9±5 |
| | | Max | 20.0±5 | 81.3±6 | 120.7±4 | 6.4±2 | 104.4±3 | 109.1±3 | -20.1±2 | 31.5±2 | 4.0±4 |
| | | ROM | 37.1±5 | 42.3±4 | 60.6±6 | 27.5±3 | 36.3±5 | 20.6±3 | 21.0±3 | 31.3±4 | 30.0±3 |

Rx, y, z: Rotation along x-, y- and z-axes

ES: Elevating stroke, trials = 3 strokes from each of 2 individuals (total 6 strokes)

SS: Scratching stroke, trials=3 stroked from each of 3 individuals (total 9 strokes)

Table 3.1. Stride parameters and shoulder joint movements (mean \pm s.e.m) during four gait cycles for each of three individuals (12 cycles total). Rx, rotation along x- axis (abduction/adduction); Ry, rotation along y-axis (extension/flexion); Rz, rotation along z-axis (supination/pronation); ROM, range of motion (max angle – min angle)

| Stride parameters | | | | | | Shoulder joint angle | | | |
|--------------------|---------------------|-------------------|--------------------------|------------------------|-----------------|----------------------|----------------|-----------------|-----------------|
| Velocity (cm/s) | Contact time (s) | Swing time (s) | Stride length (cm) | Stride freq (Hz) | Duty factor | Rx | Ry | Rz | |
| 18.4 \pm 2.0 | 0.09 \pm 0.01 | 0.07 \pm 0.01 | 2.8 \pm 0.2 | 6.4 \pm 0.4 | 0.56 \pm 0.02 | Max | 9.7 \pm 1.4 | 108.9 \pm 1.7 | 122.1 \pm 2.7 |
| | | | | | | Min | -5.0 \pm 2.5 | 61.9 \pm 2.8 | 93.9 \pm 1.9 |
| | | | | | | ROM | 14.6 \pm 1.8 | 47.0 \pm 3.3 | 28.2 \pm 1.4 |

APPENDIX B

TABLES ASSOCIATED WITH EACH CHAPTER

Figure 1.1. Study system. (A) Three-dimensional representation of the forelimb of an Eastern mole. (B) Geographical distributions and forelimb morphologies of Eastern moles (orange) and Hairy-tailed mole (blue). Sixth digit is marked in black.

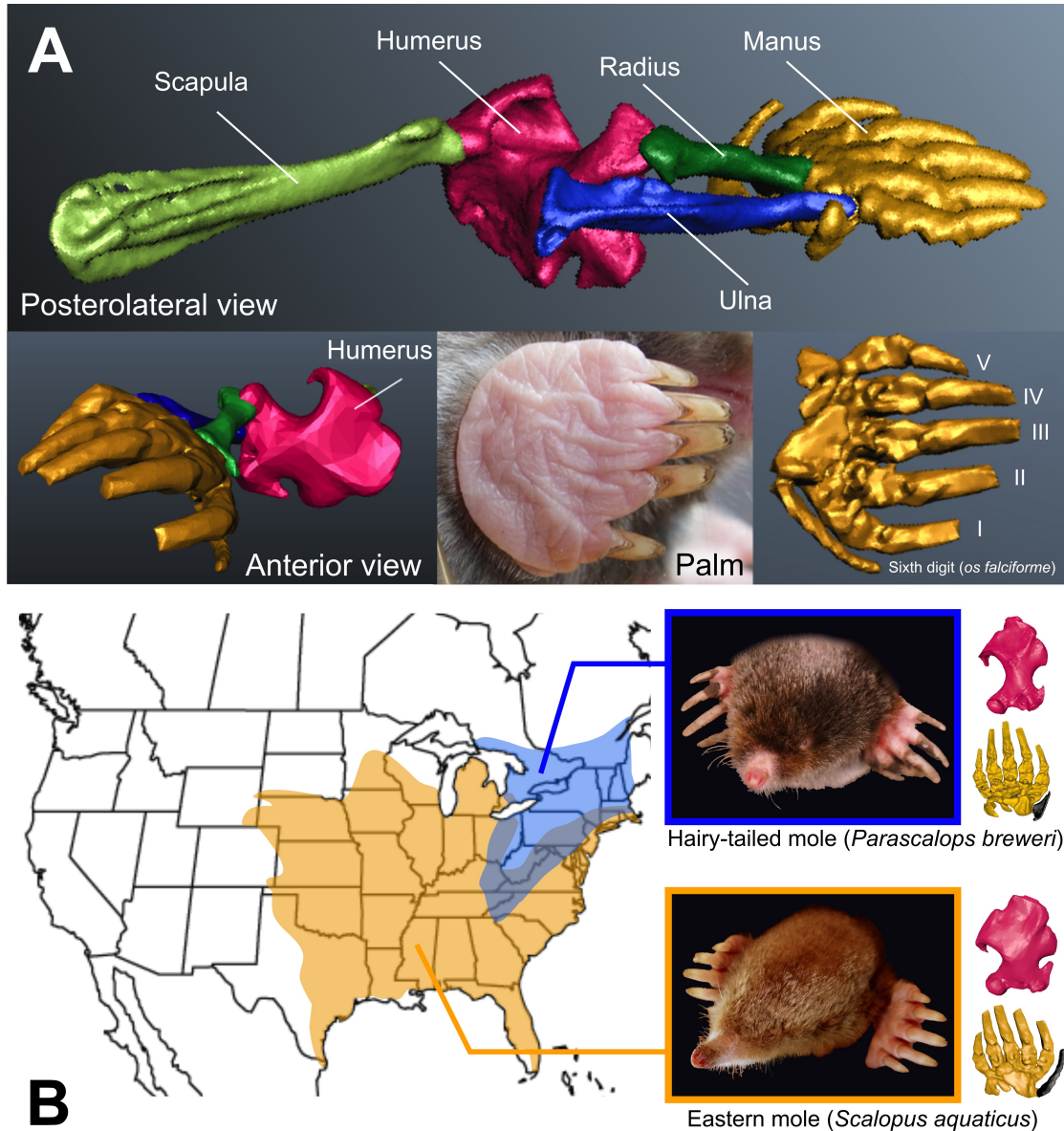


Figure 1.2. Experimental setups. Burrowing tank and wooden rods used document the speed of burrowing (A) and tendency to burrow continuously over a long distance (C). “Mole farm” (B) used to document soil transport, tunnel construction and activity level during two-hour experiments.

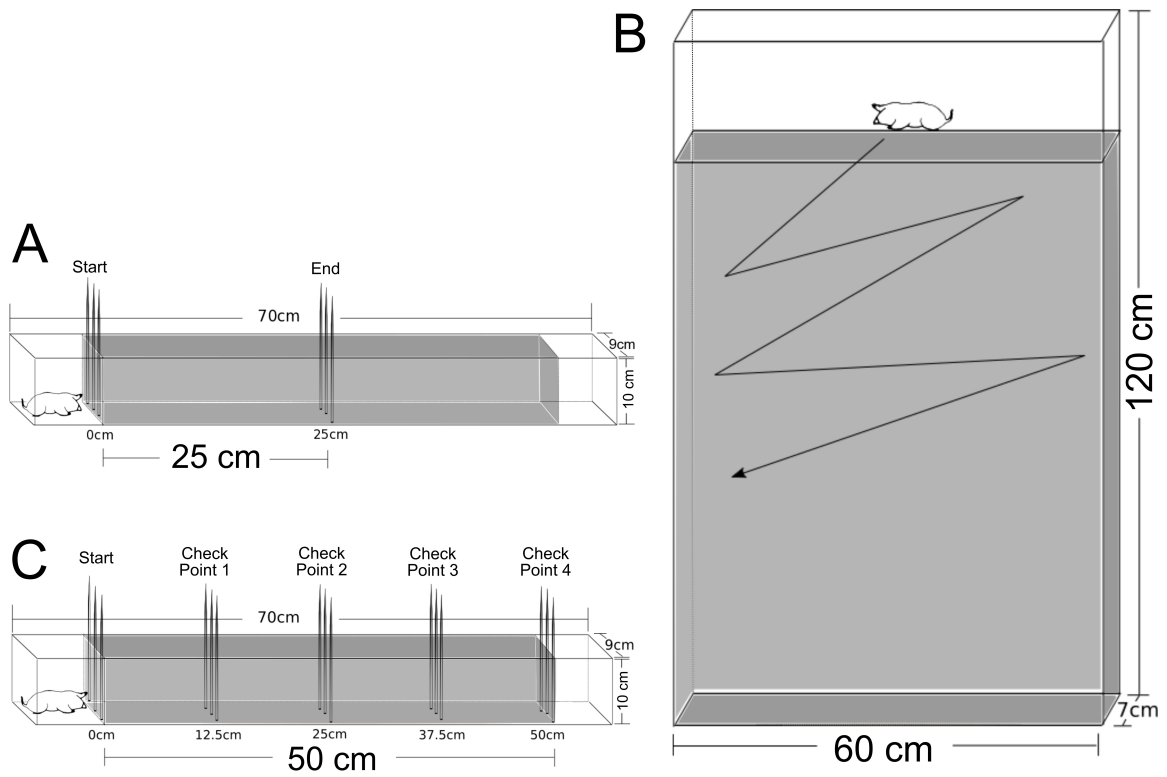


Figure 1.3. Soil compactness and the depth range of tunnel systems in Eastern and Hairy-tailed moles. Soil compactness was measured at 10cm intervals in four test pits for each species within the habitats where moles were caught. Gray bars illustrate the depth range for surface and deep tunnels observed in Eastern moles (Arlton, 1936; Harvey, 1976) and Hairy-tailed moles (Eadie, 1939).

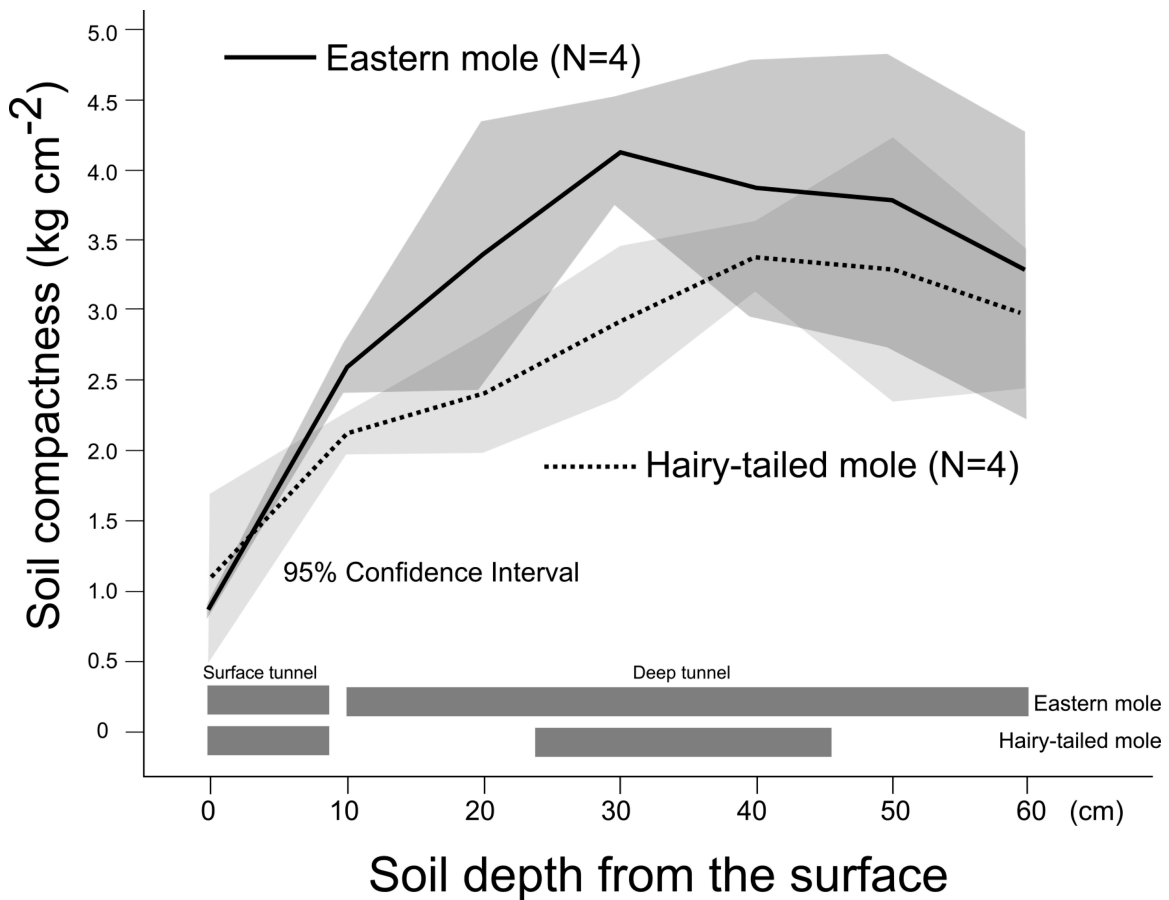


Figure 1.4. Mole burrowing speed. (A) Burrowing speed from multiple trials of six Eastern and four Hairy-tailed moles. (B) Boxplot based on maximum burrowing speed for each individual. Horizontal line represents the median. Boxes represent the 25% and 75% quartiles. Whiskers represent the maximum and minimum values excluding outliers. Points are outliers that are more than $1.5 \times$ interquartile range (IQR) from the edge of the boxes.

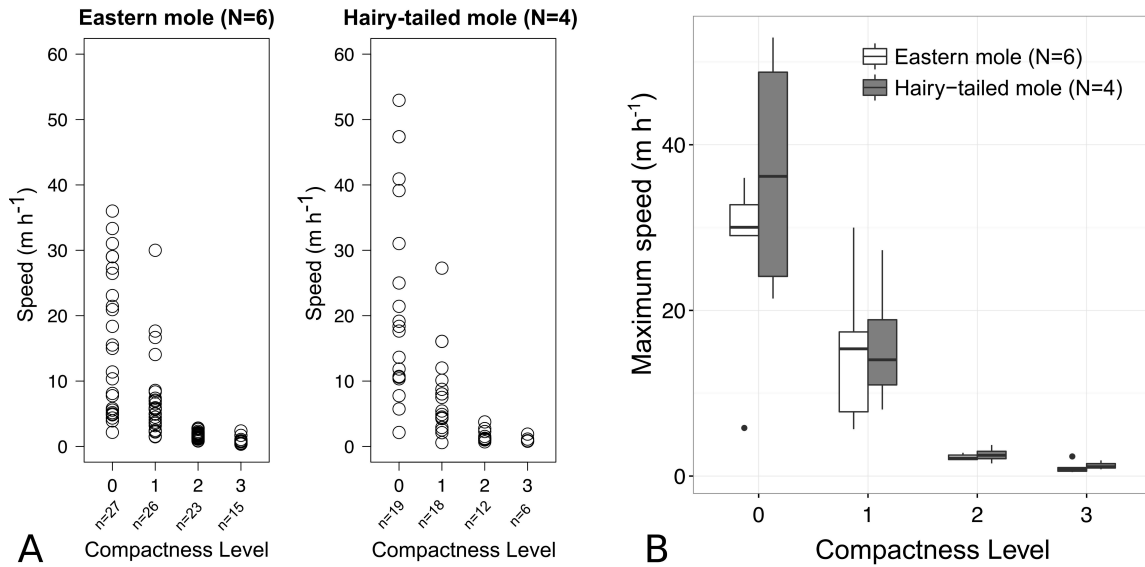


Figure 1.5. Soil transport during tunnel construction. (A) The weight of moved soil divided by the body mass of the animals for each compactness level. (B) The length of tunnel built within two hours by compactness level. (C) The proportion of time and pattern that animals were active. The total active time (capital t) for each individual is listed next to each bar. (D) The total active time of two species within two hours. All differences were based on a Tukey HSD post hoc. One asterisk represents $P < 0.05$; two asterisks represent $P < 0.01$.

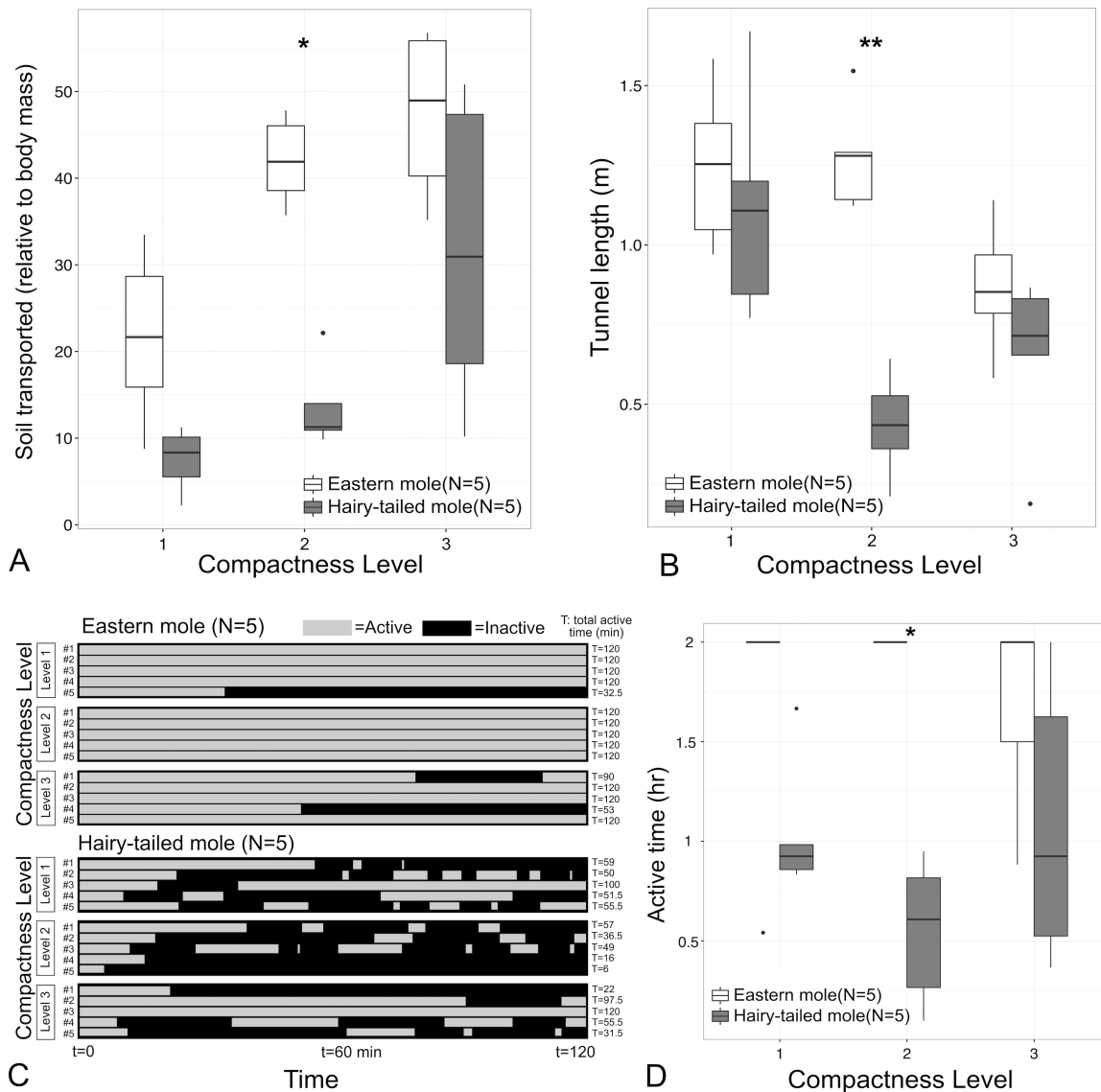


Figure 1.6. Tendency to burrow over a long distance. Completion rate by distance. Sample size (n) indicates the sum of best four trials for 6 Eastern and 4 Hairy-tailed moles.

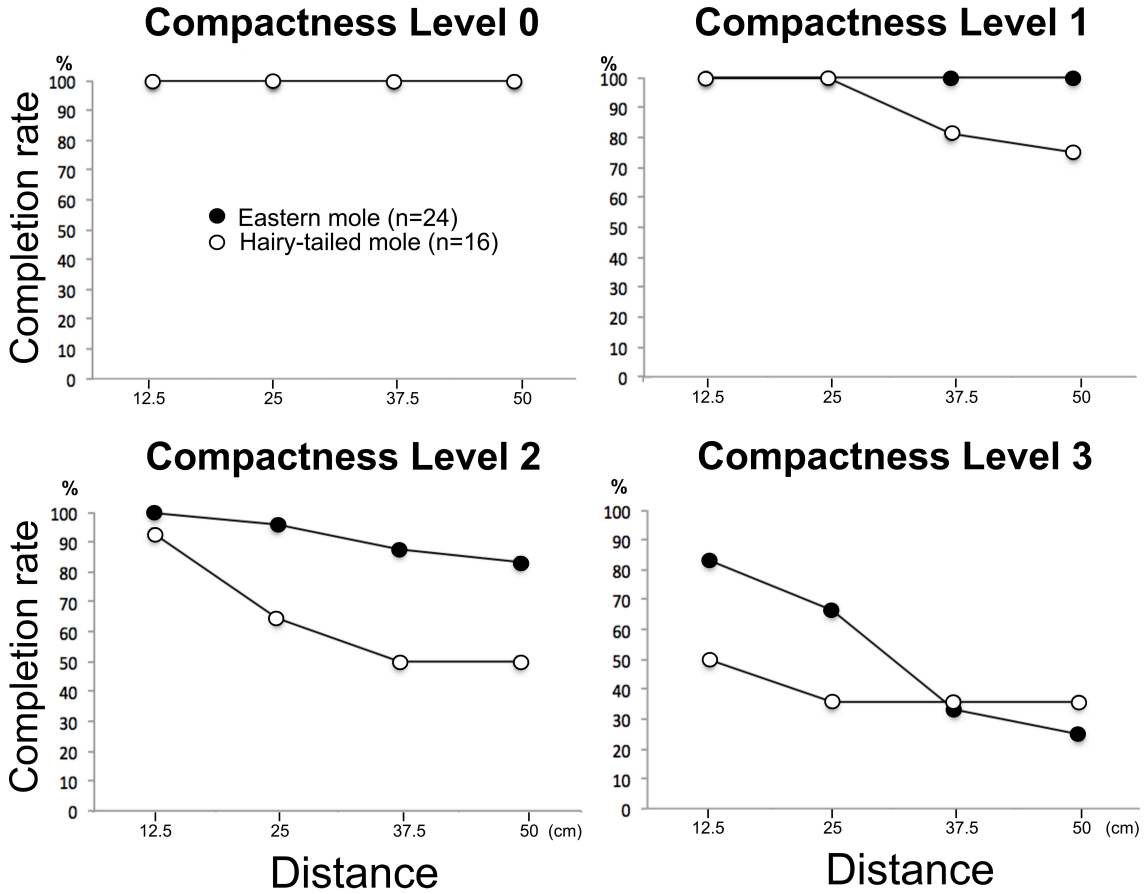


Figure 2.1. Morphological specializations of the mole forelimb. (A) The comparison of forelimb skeleton (black) between fossorial mole rats and moles (re-drawn from (Gambaryan et al., 2005) and (Gambaryan et al., 2002), respectively). (B) Right forelimb skeleton of Eastern mole (*Scalopus aquaticus*). Humerus is widened and flattened. Elliptical humeral head (white cross) is posteriorly directed and articulated with scapular glenoid fossa. Profound ulna notch rotates along the axis of humeral trochlear (asterisk).

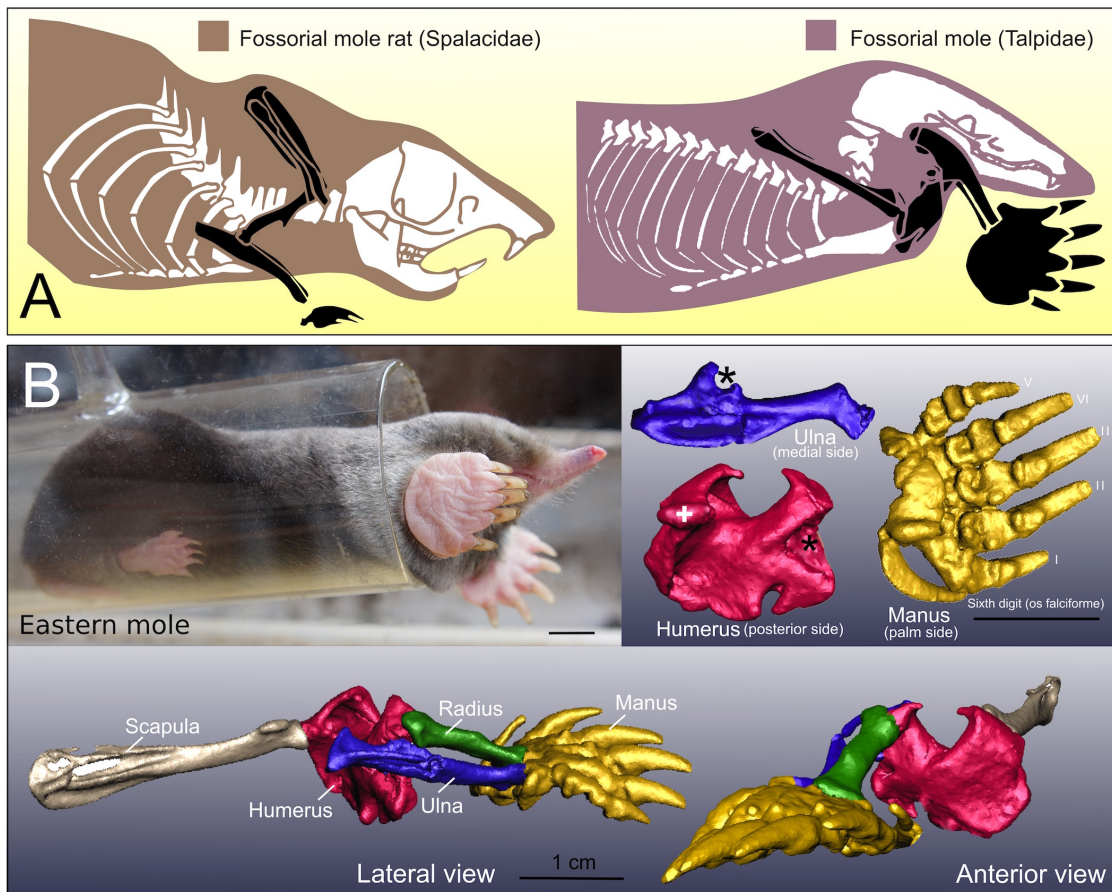


Figure 2.2. Two distinct burrowing behaviors of Eastern moles. Moles dig surface tunnels in loose soil to hunt for food at ground level. Surface tunnels are easily visible as branching raised dikes on the surface of the ground. In contrast, moles dig deep tunnels in compact soil to access underground nesting chambers. Since deep soil is compact and hard to displace, moles move this deep soil to the surface, where it can be seen as mole hills.

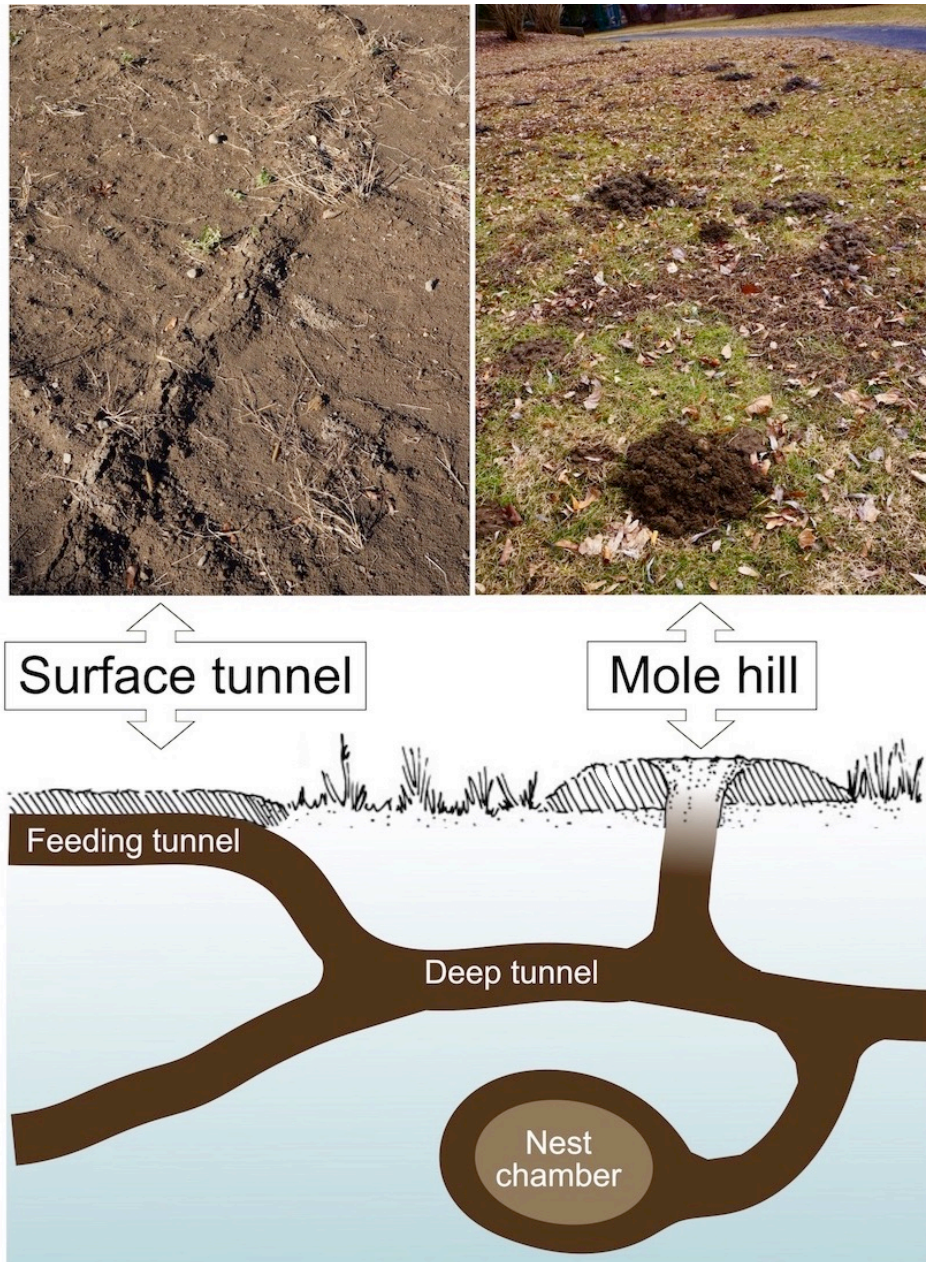


Figure 2.3. Makers and methods used for kinematic analysis. (A) and (B) show original X-ray video images of the Eastern moles from a dorsal and lateral view, respectively. Asterisk indicates the snout of mole. White crosses indicate the end of right (+) and left (+') scapula. White arrow indicates the long axis of sternum. In (C) and (D), bone models are superimposed on the X-ray frames using X-ray reconstruction of moving morphology (XROMM). Parasagittal plane (blue outline) is aligned with the long-axis of sternum. (E) Anatomical coordinate system (ACS) used to measure the trajectory of claw-tip (black sphere). The horizontal plane (green) is parallel to the ground surface. The parasagittal plane (blue) is aligned with the long-axis of the sternum over time. (F) Joint coordinate systems (JCSs) used to measure the rotations of shoulder, elbow and wrist joints. The numbers illustrate the defined joint angles in the current forelimb posture.

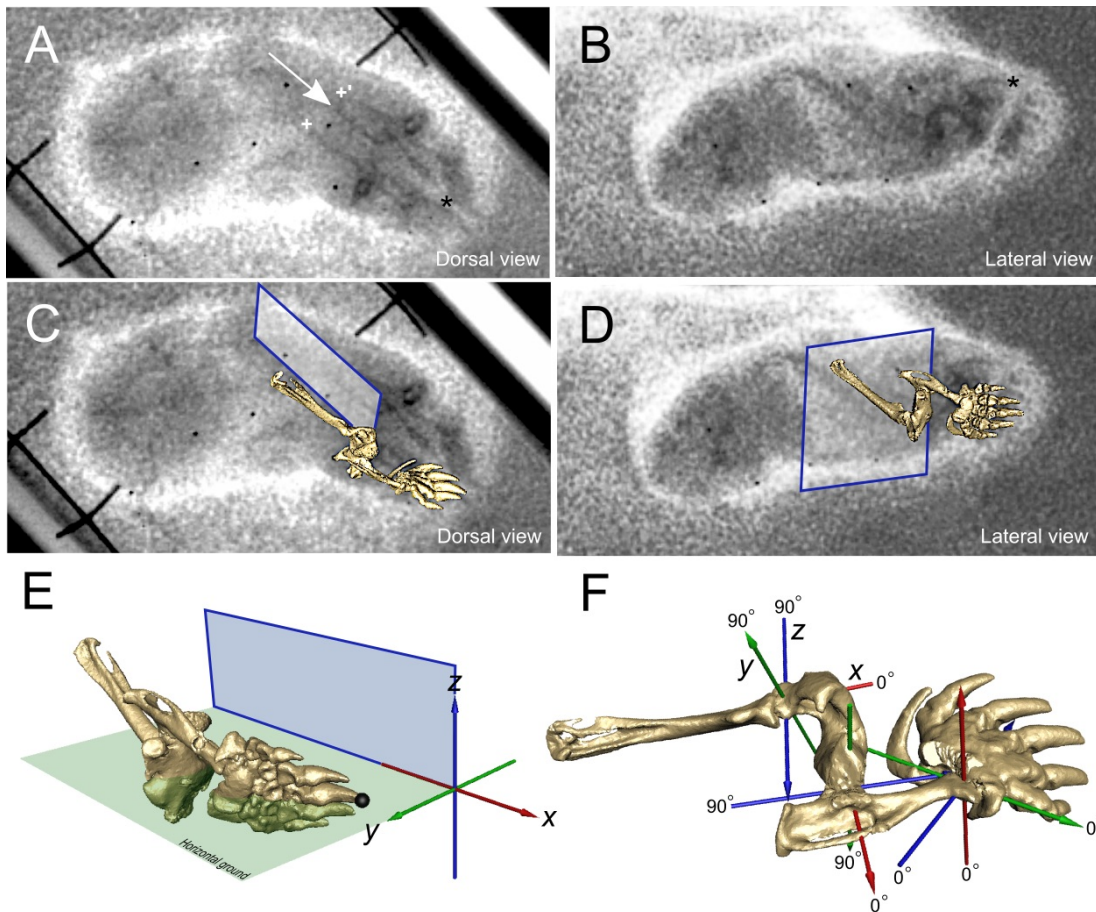


Figure 2.4. The displacements of claw-tip over a full stroke cycle. Mean (\pm s.e.m.) of translations of claw-tip for each individual during elevating and scratching strokes. The beginning of the stroke retraction occurs at 0% of the cycle. Vertical dottedlines indicate the beginning of stroke protraction. Arrows indicate the directions of the movements that would help loosening and removing soil.

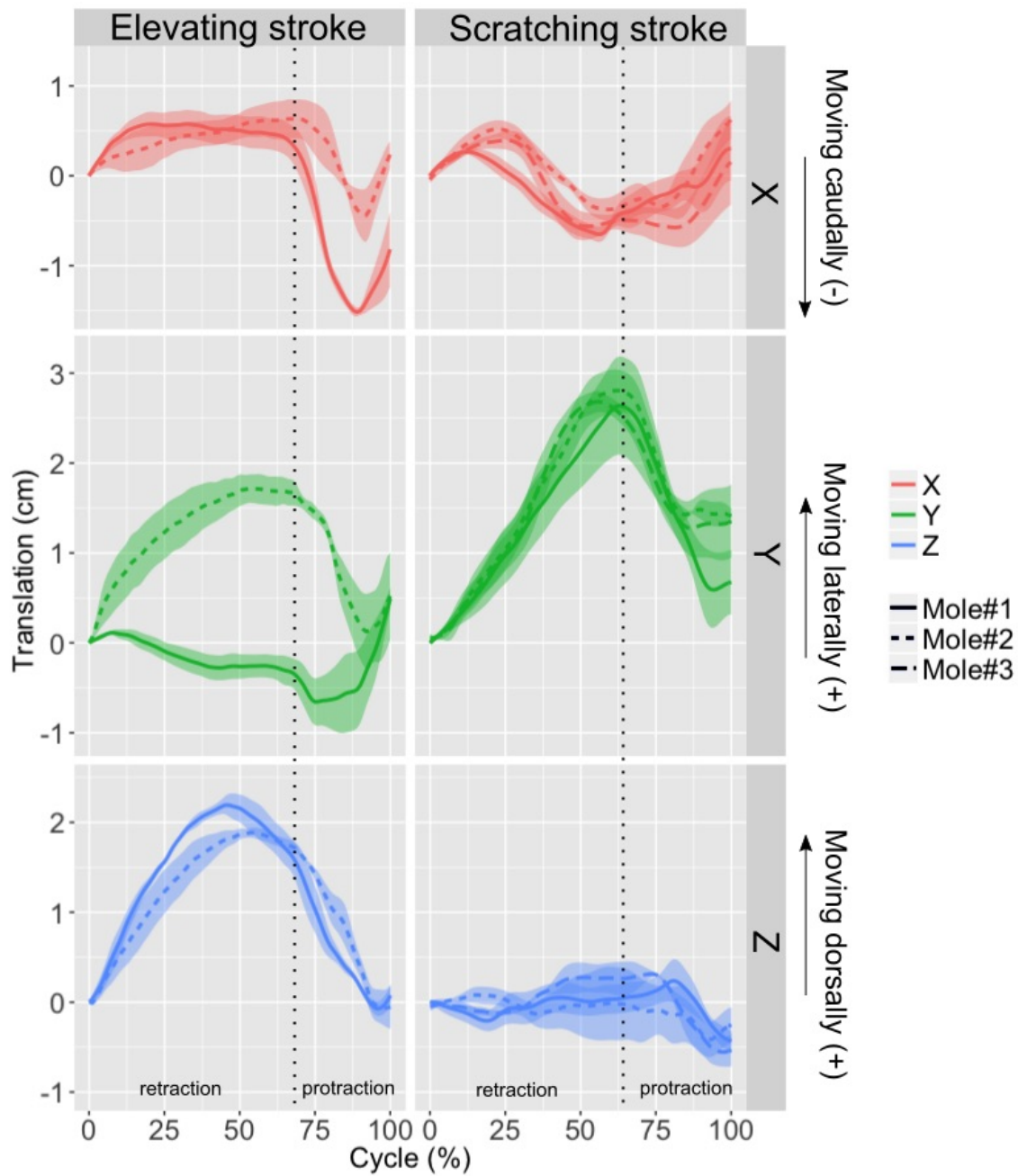


Figure 2.5. Rotation of forelimb joints. Mean (\pm s.e.m.) of rotations of the distal bone relative to its proximal bone for each individual during elevating and scratching strokes. Distal bones (humerus, ulna and manus) rotate relative to proximal bones (scapula, humerus and ulna) along x- (red), y- (green) and z- (blue) axes at shoulder (A), elbow (B) and wrist (C) joints. The beginning of the stroke retraction occurs at 0% of the cycle. Vertical dotted lines indicate the beginning of stroke protraction. Arrows indicate the movements that would help loosening and removing soil. The corresponding motion is shown in the right panel.

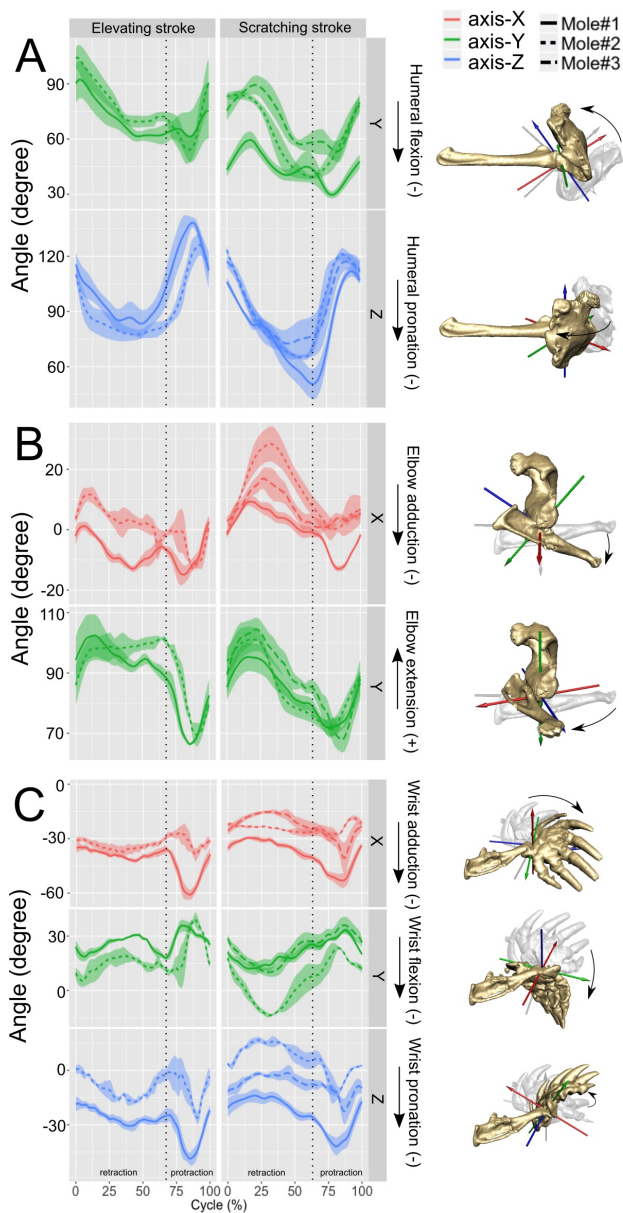


Figure 3.1. Humeral excursion and hand (manus) orientation during walking differs between moles and other terrestrial mammals. Humeral movements ranges are illustrated as excursion arcs around the shoulder joint (light blue) relative to the horizontal plane in small mammals (Jenkins, 1971) and moles (this study). The mole manus (gold) faces laterally with the “false thumb” (an enlarged sesamoid bone, sometimes called the sixth digit) lateral to the thumb (digit I).

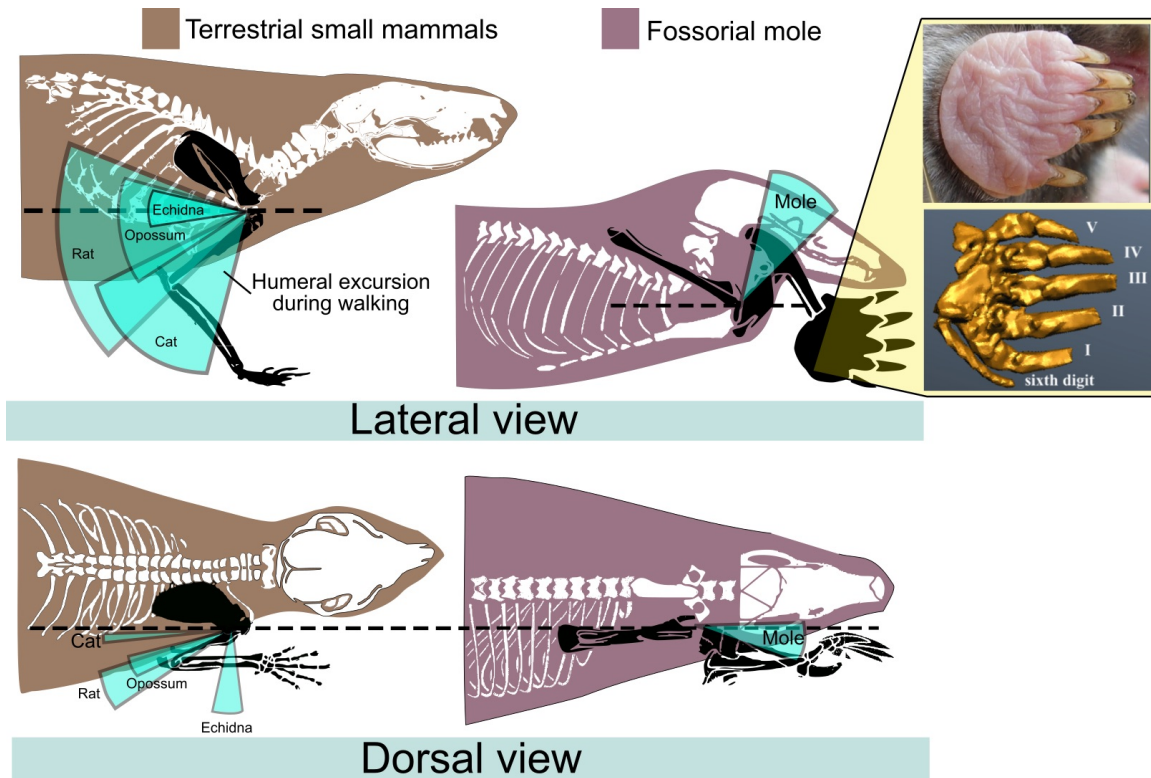
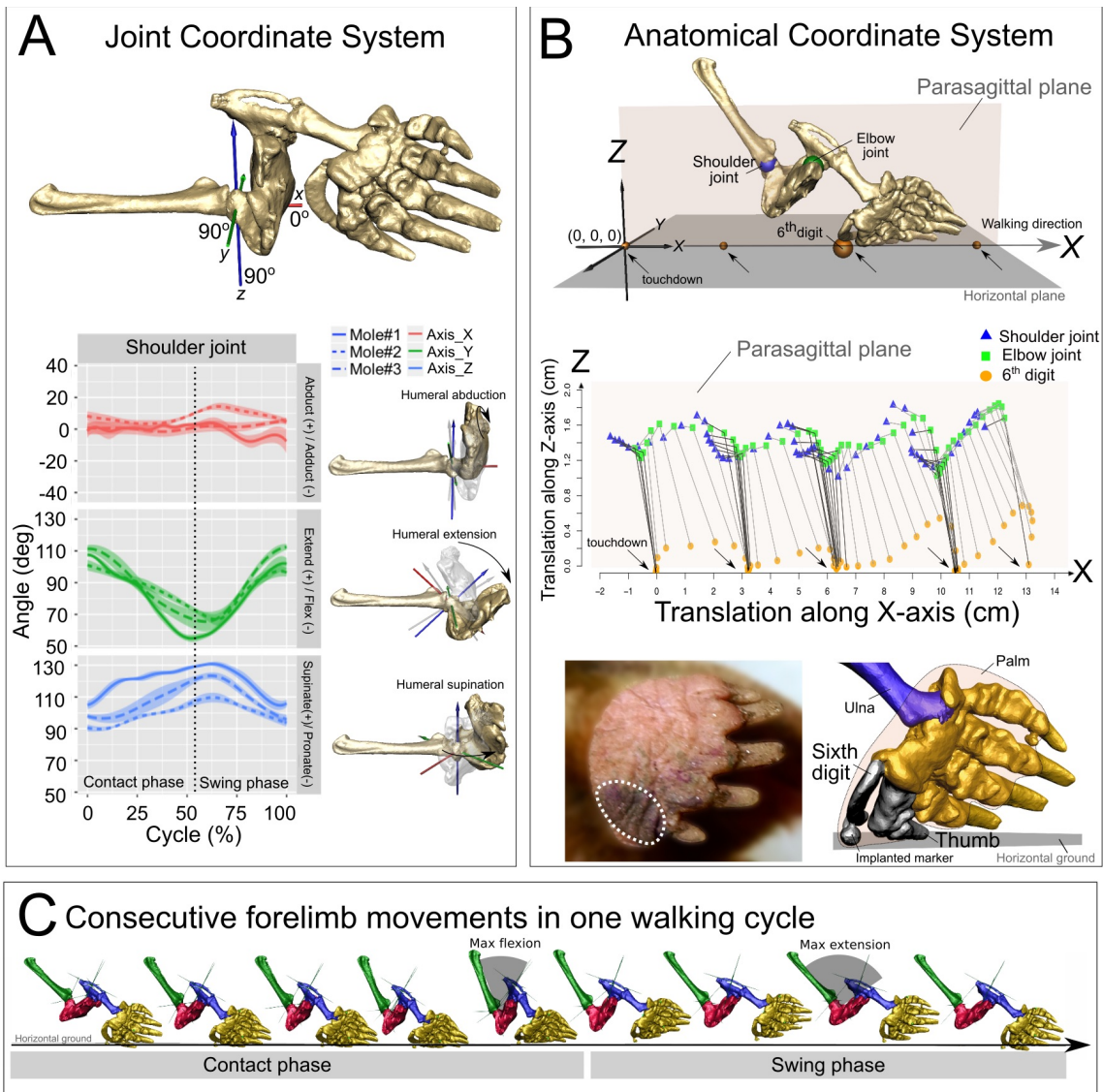


Figure 3.2. Forelimb kinematics during walking. (A) Joint coordinate system of humeral movements during mole walking. Humerus movements relative to scapula are described along x- (red, abduction+/adduction-), y- (green, extension+/flexion-), and z-axes (blue, supination+/pronation-). The “false thumb” touches down at 0% of the cycle. Dotted line indicates toe-off. (B) Displacements of the shoulder (blue sphere) and elbow (green sphere) joints and the pivot (orange sphere) of the “false thumb” in the anatomical coordinate system. The coordinate system x-axis is aligned with the walking direction

and the y-axis with the ground. Middle panel: Locations of each joint/pivot in the x- and z-axes projected onto to the parasagittal plane (light orange plane in the top panel) during movement along the x-axis. Arrows indicate “false thumb” touchdowns and beginning of the contact phase. Bottom panel: White broken circle represents the area of mole palm that touched the inkpad on the ground during mole walking. Bones that make ground-contact are colored black. (C) Forelimb movements during a walking cycle. Gray arcs illustrate peak shoulder flexion and extension. Scapula (green), humerus (red), ulna (blue) and manus (gold) are marked by different colors.



BIBLIOGRAPHY

- Alexander, R. M.** (2003). *Principles of Animal Locomotion*. Princeton, NJ, USA: Princeton University Press.
- Arlton, A. V.** (1936). An ecological study of the mole. *J. Mammal.* **17**, 349–371.
- Astley, H. C. and Roberts, T. J.** (2012). Evidence for a vertebrate catapult: elastic energy storage in the plantaris tendon during frog jumping. *Biol. Lett.* **8**, 386–9.
- Astley, H. C. and Roberts, T. J.** (2014). The mechanics of elastic loading and recoil in anuran jumping. *J. Exp. Biol.* **217**, 4372–4378.
- Baier, D. B. and Gatesy, S. M.** (2013). Three-dimensional skeletal kinematics of the shoulder girdle and forelimb in walking Alligator. *J. Anat.* **223**, 462–73.
- Baier, D. B., Gatesy, S. M. and Jenkins, F. A. J.** (2007). A critical ligamentous mechanism in the evolution of avian flight. *Nature* **445**, 307–10.
- Baier, D. B., Gatesy, S. M. and Dial, K. P.** (2013). Three-dimensional, high-resolution skeletal kinematics of the avian wing and shoulder during ascending flapping flight and uphill flap-running. *PLoS One* **8**, e63982.
- Bakker, R. T.** (1971). Dinosaur physiology and the origin of mammals. *Evolution (N. Y.)* **25**, 636–658.
- Biewener, A. A.** (1983). Allometry of quadrupedal locomotion: the scaling of duty factor, bone curvature and limb orientation to body size. *J. Exp. Biol.* **105**, 147–171.
- Biewener, A.** (1989). Scaling body support in mammals: limb posture and muscle mechanics. *Science* **245**, 45–48.
- Biewener, A. A.** (1990). Biomechanics of mammalian terrestrial locomotion. *Science* **250**, 1097–103.
- Biewener, A. A.** (2006). Patterns of mechanical energy change in tetrapod gait: pendula, springs and work. *J. Exp. Zool. A. Comp. Exp. Biol.* **305**, 899–911.
- Brainerd, E. L., Baier, D. B., Gatesy, S. M., Hedrick, T. L., Metzger, K. a, Gilbert, S. L. and Crisco, J. J.** (2010). X-ray reconstruction of moving morphology (XROMM): precision, accuracy and applications in comparative biomechanics research. *J. Exp. Zool. A. Ecol. Genet. Physiol.* **313**, 262–79.
- Camp, A. L. and Brainerd, E. L.** (2014). Role of axial muscles in powering mouth expansion during suction feeding in largemouth bass (*Micropterus salmoides*). *J. Exp. Biol.* **217**, 1333–45.
- Camp, A. L., Roberts, T. J. and Brainerd, E. L.** (2015). Swimming muscles power suction feeding in largemouth bass. *Proc. Natl. Acad. Sci. U. S. A.* **112**, 8690–5.

- Campbell, B.** (1939). The shoulder anatomy of the moles. A study in phylogeny and adaptation. *Am. J. Anat.* **64**, 1–39.
- Carraway, L. N. and Verts, B. J.** (1991). *Neurotrichus gibbsii*. *Mamm. Species* **1880**, 1–7.
- Charig, A. J.** (1972). The evolution of the archosaur pelvis and hindlimb: an explanation in functional terms. In *Studies in Vertebrate Evolution* (ed. Joysey, K. A.) and Kemp, T. S.), pp. 121–155. Edinburgh: Oliver & Boyd.
- Crompton, A. W. and Jenkins, F. A., J.** (1973). Mammals from reptiles: a review of mammalian origins. *Annu. Rev. Earth Planet. Sci.* **1**, 131–155.
- Dalquest, W. W. and Orcutt, D. R.** (1942). The biology of the least shrew-mole, *Neurotrichus gibbsii minor*. *Am. Midl. Nat.* **27**, 387–401.
- Dawson, M. M., Metzger, K. A., Baier, D. B. and Brainerd, E. L.** (2011). Kinematics of the quadrate bone during feeding in mallard ducks. *J. Exp. Biol.* **214**, 2036–46.
- Eadie, W.** (1939). A contribution to the biology of *Parascalops breweri*. *J. Mammal.* **20**, 150–173.
- Ebensperger, L. a and Bozinovic, F.** (2000). Energetics and burrowing behaviour in the semifossorial degu *Octodon degus* (Rodentia: Octodontidae). *J. Zool. London* **252**, 179–186.
- Edwards, L. F.** (1937). Morphology of the forelimb of the mole (*Scalops aquaticus*, L.) in relation to its fossorial habits. *Ohio J. Sci.* **37**, 20–41.
- Edwards, C. A. and Bohlen, P. J.** (1996). *Biology and Ecology of Earthworms*. 3rd editio. London, UK: Chapman & Hall.
- Farley, C. T. and Ko, T. C.** (1997). Mechanics of locomotion in lizards. *J. Exp. Biol.* **200**, 2177–2188.
- Fraser, E. E. and Miller, J. F.** (2008). Diurnal above-ground movement in Hairy-tailed Moles, *Parascalops breweri*. *Can. Field-Naturalist* **122**, 267.
- Freeman, R. A.** (1886). Anatomy of the shoulder and upper arm of the mole (*Talpa europaea*). *J. Anat. Physiol.* **20**, 201–219.
- Full, R. J., Zuccarello, D. A. and Tullis, A.** (1990). Effect of variation in form on the cost of terrestrial locomotion. *J. Exp. Biol.* **150**, 233–246.
- Gambaryan, P. P.** (2002). Evolution of tetrapod locomotion. *Zh. Obshch. Biol.* **63**, 426–445.
- Gambaryan, P. P. and Kuznetsov, A. N.** (2013). An evolutionary perspective on the walking gait of the long-beaked echidna. *J. Zool.* **290**, 58–67.

- Gambaryan, P. P., Gasc, J. P. and Renous, S.** (2002). Cinefluorographical study of the burrowing movements in the common mole, *Talpa europaea* (Lipotyphla, Talpidae). *Russ. J. Theriol.* **1**, 91–109.
- Gatesy, S. M., Baier, D. B., Jenkins, F. a and Dial, K. P.** (2010). Scientific rotoscoping: a morphology-based method of 3-D motion analysis and visualization. *J. Exp. Zool. A. Ecol. Genet. Physiol.* **313**, 244–261.
- Gidmark, N. J., Staab, K. L., Brainerd, E. L. and Hernandez, L. P.** (2012). Flexibility in starting posture drives flexibility in kinematic behavior of the kinethmoid-mediated premaxillary protrusion mechanism in a cyprinid fish, *Cyprinus carpio*. *J. Exp. Biol.* **215**, 2262–72.
- Gorman, M. L. and Stone, R. D.** (1990). *The natural history of moles*. London: Christopher Helm Ltd /A and C Black, London and Cornell University Press.
- Graves, G. R.** (2002). Crepuscular surface foraging of the hairy-tailed mole (*Parascalops breweri*). *J. North Carolina Acad. Sci.* **118**, 206–209.
- Gregory, W. K.** (1912). Notes on the principles of quadrupedal locomotion and the mechanism of the limbs in hoofed animals. *Ann. N. Y. Acad. Sci.* **22**, 267–294.
- Hallett, J. G.** (1978). *Parascalops breweri*. *Mamm. Species* 1.
- Hamilton, W. J. J.** (1931). Habits of the Star-nosed mole, *Condylura cristata*. *J. Mammal.* **12**, 345–355.
- Hamilton, W. J.** (1939). Activity of Brewer’s mole (*Parascalops breweri*). *J. Mammal.* **20**, 307–310.
- NatureServe (Hammerson, G.)** (2008). *Parascalops breweri*. The IUCN Red List of Threatened Species 2008: e.T41469A 10477508. doi: 10.2305/IUCN.UK.2008.RLTS.T41469A 10477508.en.
- Hartman, G. D. and Yates, T. L.** (1985). *Scapanus orarius*. *Mamm. Species* 1–5.
- Harvey, M. J.** (1976). Home range, movements, and diel activity of the Eastern mole, *Scalopus aquaticus*. *Am. Midl. Nat.* **95**, 436–445.
- Hedrick, T. L., Tobalske, B. W., Ros, I. G., Warrick, D. R. and Biewener, A. A.** (2012). Morphological and kinematic basis of the hummingbird flight stroke: scaling of flight muscle transmission ratio. *Proc. Biol. Sci.* **279**, 1986–92.
- Heglund, N. C., Cavagna, G. a and Taylor, C. R.** (1982). Energetics and mechanics of terrestrial locomotion. III. Energy changes of the centre of mass as a function of speed and body size in birds and mammals. *J. Exp. Biol.* **97**, 41–56.
- Hickman, G. C. and Brown, L. N.** (1973). Pattern and rate of mound production in the southeastern Pocket gopher (*Geomys pinetis*). *J. Mammal.* **54**, 971–975.

- Hisaw, F. L.** (1923). Observations on the burrowing habits of moles (*Scalopus aquaticus machrinoides*). *J. Mammal.* **4**, 79–88.
- Hutchinson, J. R., Delmer, C., Miller, C. E., Hildebrandt, T., Pitsillides, A. A. and Boyde, A.** (2011). From flat foot to fat foot: structure, ontogeny, function, and evolution of elephant “sixth toes”. *Science* **334**, 1699–703.
- Jarvis, J. U. M. and Sale, J. B.** (1971). Burrowing and burrow patterns of East African mole-rats *Tachyoryctes*, *Heliophobius* and *Heterocephalus*. *J. Zool. London* **163**, 451–479.
- Jenkins, F. A.** (1970). Limb movements in a monotreme (*Tachyglossus aculeatus*): a cineradiographic analysis. *Science* **168**, 1473–1475.
- Jenkins, F.** (1971). Limb posture and locomotion in the Virginia opossum (*Didelphis marsupialis*) and in other non-cursorial mammals. *J. Zool.* **165**, 303–315.
- Jenkins, F. A. and Goslow, G. E.** (1983). The functional anatomy of the shoulder of the Savannah Monitor lizard (*Varanus exanthematicus*). *J. Morphol.* **175**, 195–216.
- Jensen, I. M.** (1983). Metabolic Rates of the Hairy-Tailed Mole, *Parascalops breweri* (Bachman, 1842). *J. Mammal.* **64**, 453–462.
- Jensen, I. M.** (1986a). Foraging strategies of the mole (*Parascalops breweri*, Bachman, 1842). I. The distribution of prey. *Can. J. Zool.* **64**, 1727–1733.
- Jensen, I. M.** (1986b). Foraging strategies of the mole (*Parascalops breweri*, Bachman, 1842). II. The economics of finding prey. *Can. J. Zool.* **64**, 1734–1738.
- Kardong, K.** (1995). *Vertebrates: comparative anatomy, function, evolution*. Dubuque, IA: Wm. C. Brown Publ.
- Kley, N. J. and Kearney, M.** (2007). Adaptations for digging and burrowing. In *Fins into Limbs: Evolution, Development, and Transformation* (ed. Hall, B. K.), pp. 284–309. Chicago, IL, USA: University of Chicago Press.
- Knörlein, B. J., Baier, D. B., Gatesy, S. M., Laurence-Chasen, J. D. and Brainerd, E. L.** (2016). Validation of XMALab software for marker-based XROMM. *J. Exp. Biol.* jeb.145383.
- Konow, N., Cheney, J. a, Roberts, T. J., Waldman, J. R. S. and Swartz, S. M.** (2015). Spring or string: does tendon elastic action influence wing muscle mechanics in bat flight? *Proc. R. Soc. B Biol. Sci.* **282**, 1–7.
- Laundré, J. W. and Reynolds, T. D.** (1993). Effects of soil structure on burrow characteristics of five small mammal species. *West. North Am. Nat.* **53**, 358–366.
- Lin, Y.-F., Chappuis, A., Rice, S. and Dumont, E. R.** (2017). The effects of soil compactness on the burrowing performance of sympatric eastern and hairy-tailed moles. *J. Zool.* **301**, 310–319.

- Lovegrove, B. G.** (1989). The cost of burrowing by the social mole rats (Bathyergidae) *Cryptomys damarensis* and *Heterocephalus glaber*: the role of soil moisture. *Physiol. Zool.* **62**, 449–469.
- Luna, F. and Antinuchi, C. D.** (2006). Cost of foraging in the subterranean rodent *Ctenomys talarum*: effect of soil hardness. *Can. J. Zool. Can. Zool.* **84**, 661–667.
- Mason, M. J.** (2006). Middle ear structures in fossorial mammals: a comparison with non-fossorial species. *J. Zool.* **255**, 467–486.
- McNab, B. K.** (1979). The influence of body size on the energetics and distribution of fossorial and burrowing mammals. *Ecology* **60**, 1010–1021.
- Miller, R. G.** (1981). *Simultaneous Statistical Inference*. New York, NY, USA: Springer.
- Mitgutsch, C., Richardson, M., Jiménez, R., Martin, J. E., Kondrashov, P., de Bakker, M. A. G. and Sánchez-Villagra, M. R.** (2012). Circumventing the polydactyly “constraint”: the mole’s “thumb.” *Biol. Lett.* **8**, 74–77.
- Nevo, E.** (1979). Adaptive convergence and divergence of subterranean mammals. *Ann. Rev. Ecol. Syst.* **10**, 269–308.
- O’Neill, M. C., Lee, L. F., Demes, B., Thompson, N. E., Larson, S. G., Stern, J. T. and Umberger, B. R.** (2015). Three-dimensional kinematics of the pelvis and hind limbs in chimpanzee (*Pan troglodytes*) and human bipedal walking. *J. Hum. Evol.* **86**, 32–42.
- Panagiotopoulou, O., Pataky, T. C., Day, M., Hensman, M. C., Hensman, S., Hutchinson, J. R. and Clemente, C. J.** (2016). Foot pressure distributions during walking in African elephants (*Loxodonta africana*). *R. Soc. open sci.* **3**, 160203.
- Petersen, K. E. and Yates, T. L.** (1980). *Condylura cristata*. *Mamm. Species* **5**, 1–4.
- Pierce, S. E., Clack, J. a and Hutchinson, J. R.** (2012). Three-dimensional limb joint mobility in the early tetrapod *Ichthyostega*. *Nature* **486**, 523–6.
- Pierce, S. E., Hutchinson, J. R. and Clack, J. A.** (2013). Historical perspectives on the evolution of tetrapodomorph movement. *Integr. Comp. Biol.* **53**, 209–223.
- Piras, P., Sansalone, G., Teresi, L., Kotsakis, T., Colangelo, P. and Loy, A.** (2012). Testing convergent and parallel adaptations in talpids humeral mechanical performance by means of geometric morphometrics and finite element analysis. *J. Morphol.* **273**, 696–711.
- Reed, C. A.** (1951). Locomotion and appendicular anatomy in three Soricoid insectivores. *Am. Midl. Nat.* **45**, 513–671.
- Riskin, D. K. and Hermanson, J. W.** (2005). Biomechanics: independent evolution of running in vampire bats. *Nature* **434**, 292.

- Rose, J. A., Sandefur, M., Huskey, S., Demler, J. L. and Butcher, M. T.** (2013). Muscle architecture and out-force potential of the thoracic limb in the eastern mole (*Scalopus aquaticus*). *J. Morphol.* **274**, 1277–1287.
- Sánchez-Villagra, M. R. and Menke, P. R.** (2005). The mole's thumb — evolution of the hand skeleton in talpids (Mammalia). *Zoology* **108**, 3–12.
- Sánchez-Villagra, M. R., Horovitz, I. and Motokawa, M.** (2006). A comprehensive morphological analysis of talpid moles (Mammalia) phylogenetic relationships. *Cladistics* **22**, 59–88.
- Seymour, R. S., Withers, P. C. and Weathers, W. W.** (1998). Energetics of burrowing, running, and free-living in the Namib Desert golden mole (*Eremitalpa namibensis*). *J. Zool.* **244**, 107–117.
- Skoczen, S.** (1958). Tunnel digging by the mole (*Talpa Europaea* Linne). *Acta Theriol. (Warsz)*. **2**, 235–249.
- Stein, B. R.** (2000). Morphology of subterranean rodents. In *Life Underground: The Biology of Subterranean Rodents* (ed. Lacey, E. A.), Patton, J. L.), and Cameron, G. N.), pp. 19–61. Chicago and London: The university of Chicago.
- Taylor, C. R., Schmidt-Nielsen, K. and Raab, J. L.** (1970). Scaling of energetic cost of running to body size in mammals. *Am. J. Physiol.* **219**, 1104–1107.
- Vickaryous, M. K. and Olson, W. M.** (2007). Sesamoids and ossicles in the appendicular skeleton. In *Fins into Limbs: Evolution, Development, and Transformation* (ed. Hall, B. K.), p. Chicago, IL, USA: University of Chicago Press.
- Vleck, D.** (1979). The energy costs of burrowing by the pocket gopher *Thomomys bottae*. *Physiol. Zool.* **52**, 122–136.
- Vleck, D.** (1981). Burrow structure and foraging costs in the fossorial rodent, *Thomomys bottae*. *Oecologia* **49**, 391–396.
- Whidden, H. P.** (2000). Comparative myology of moles and the phylogeny of the Talpidae (Mammalia, Lipotyphla). *Am. Museum Novit.* **3294**, 1–53.
- Willey, J. S., Biknevicius, A. R., Reilly, S. M. and Earls, K. D.** (2004). The tale of the tail: limb function and locomotor mechanics in *Alligator mississippiensis*. *J. Exp. Biol.* **207**, 553–563.
- Wilson, D. E. and Reeder, D. M. eds.** (2005). *Mammal Species of the World. A Taxonomic and Geographic Reference*. 3rd ed. Baltimore, Maryland.: Johns Hopkins University.
- Wu, N. C., Alton, L. A., Clemente, C. J., Kearney, M. R. and White, C. R.** (2015). Morphology and burrowing energetics of semi-fossorial skinks (*Liopholis* spp.). *J. Exp. Biol.* **218**, 2416–2426.

- Yalden, D. W.** (1966). The anatomy of mole locomotion. *J. Zool.* **149**, 55–64.
- Yates, T. L. and Schmidly, D. J.** (1978). *Scalopus aquaticus*. *Mamm. Species* 1–4.
- Zelová, J., Šumbera, R., Okrouhlík, J. and Burda, H.** (2010). Cost of digging is determined by intrinsic factors rather than by substrate quality in two subterranean rodent species. *Physiol. Behav.* **99**, 54–58.
- Zuur, A. F., Ieno, E. N., Walker, N., Saveliev, A. A. and Smith, G. M.** (2009). *Mixed effects models and extensions in ecology with R*. New York, NY: Springer New York.